




ORIGINAL RESEARCH

Double Deletion of Angiotensin II Type 2 and Mas Receptors Accelerates Aging-Related Muscle Weakness in Male Mice

Hikari Takeshita, PhD; Koichi Yamamoto , MD, PhD; Masaki Mogi , MD, PhD; Yu Wang, BM; Yoichi Nozato, MD, PhD; Taku Fujimoto, MD, PhD; Serina Yokoyama, MD, PhD; Kazuhiro Hongyo, MD, PhD; Futoshi Nakagami, MD, PhD; Hiroshi Akasaka, MD, PhD; Yoichi Takami, MD, PhD; Yasushi Takeya, MD, PhD; Ken Sugimoto, MD, PhD; Masatsugu Horiuchi, MD, PhD; Hiromi Rakugi , MD, PhD

BACKGROUND: The activation of AT2 (angiotensin II type 2 receptor) and Mas receptor by angiotensin II and angiotensin-(1-7), respectively, is the primary process that counteracts activation of the canonical renin-angiotensin system (RAS). Although inhibition of canonical RAS could delay the progression of physiological aging, we recently reported that deletion of Mas had no impact on the aging process in mice. Here, we used male mice with a deletion of only AT2 or a double deletion of AT2 and Mas to clarify whether these receptors contribute to the aging process in a complementary manner, primarily by focusing on aging-related muscle weakness.

METHODS AND RESULTS: Serial changes in grip strength of these mice up to 24 months of age showed that AT2/Mas knockout mice, but not AT2 knockout mice, had significantly weaker grip strength than wild-type mice from the age of 18 months. AT2/Mas knockout mice exhibited larger sizes, but smaller numbers and increased frequency of central nucleation (a marker of aged muscle) of single skeletal muscle fibers than AT2 knockout mice. Canonical RAS-associated genes, inflammation-associated genes, and senescence-associated genes were highly expressed in skeletal muscles of AT2/Mas knockout mice. Muscle angiotensin II content increased in AT2/Mas knockout mice.

CONCLUSIONS: Double deletion of AT2 and Mas in mice exaggerated aging-associated muscle weakness, accompanied by signatures of activated RAS, inflammation, and aging in skeletal muscles. Because aging-associated phenotypes were absent in single deletions of the receptors, AT2 and Mas could complement each other in preventing local activation of RAS during aging.

Key Words: aging ■ angiotensin II type 2 receptor ■ Mas receptor ■ muscle ■ renin-angiotensin system

The renin-angiotensin system (RAS), primarily involved in the maintenance of blood pressure, has been identified to be functional in individual organs including skeletal muscles.¹⁻⁵ Previous studies have suggested that acute administration of angiotensin II induces muscle wasting in rodents.⁶⁻⁸ Conversely, RAS inhibition was reported to alleviate pathological conditions associated with muscle disorders, including muscular dystrophies, in mice.⁹⁻¹¹ In addition, the

contribution of RAS in aging-associated muscle weakness is supported by findings revealing that pharmacological and genetic inhibition of AT1 (angiotensin II type 1 receptor) led to protection from physiological muscle weakness, muscle injury, and disuse muscle atrophy in aged mice.^{9,12,13}

Accumulating lines of evidence have established the presence of 2 endogenous pathways that confer protection from RAS activation, namely, the ACE2

Correspondence to: Koichi Yamamoto, MD, PhD, Department of Geriatric and General Medicine, Osaka University Graduate School of Medicine, 2-2 Yamadaoka, Suita, Osaka 565-0871, Japan. E-mail: kyamamoto@geriat.med.osaka-u.ac.jp

Supplementary Material for this article is available at <https://www.ahajournals.org/doi/suppl/10.1161/JAHA.120.021030>

For Sources of Funding and Disclosures, see page 10.

© 2021 The Authors. Published on behalf of the American Heart Association, Inc., by Wiley. This is an open access article under the terms of the Creative Commons Attribution-NonCommercial-NoDerivs License, which permits use and distribution in any medium, provided the original work is properly cited, the use is non-commercial and no modifications or adaptations are made.

JAHA is available at: www.ahajournals.org/journal/jaha

CLINICAL PERSPECTIVE

What Is New?

- Double deletion, but not single deletion, of the AT2 (angiotensin II type 2 receptor) and an angiotensin-(1-7) receptor, Mas, both of which involved in protection against the activation of the renin-angiotensin system, contribute to accelerated aging-induced muscle weakness in mice.

What Are the Clinical Implications?

- AT2 and Mas could act complementarily to prevent transcriptional activation of the muscle renin-angiotensin system, thereby leading to alleviation of aging-induced muscle weakness.
- The current findings support the pivotal and complementary role of AT2 and Mas in maintaining skeletal muscle homeostasis during aging, which prevents the local activation of the renin-angiotensin system.

Nonstandard Abbreviations and Acronyms

A1-7	angiotensin 1-7
ACE2	angiotensin-converting enzyme 2
AT1	angiotensin II type 1 receptor
AT2	angiotensin II type 2 receptor
CNF	central nucleated fiber
H&E	hematoxylin and eosin
KO	knockout
RAS	renin-angiotensin system
SDH	succinate dehydrogenase
WT	wild-type

(angiotensin-converting enzyme 2)/A1-7 (angiotensin 1-7)/Mas axis and the angiotensin II/AT2 (angiotensin II type 2 receptor) axis. The protective role of A1-7 in muscle disorders, exerted by binding to Mas, has been well established by previous reports using animal models of several muscle disorders.¹⁴⁻¹⁸ However, this protective effect is not observed in aging-associated muscle weakness. We have recently reported that the absence of ACE2, which cleaves angiotensin II into A1-7, accelerates aging-associated muscle weakness because of upregulation of the senescence-associated *p16* gene and led to increased central nucleated fibers (CNFs) in mice.^{19,20} In contrast, Mas knockout (Mas KO) mice did not exhibit any phenotypes of early aging, suggesting that the early aging phenotypes of ACE2 knockout (ACE2 KO) mice were independent of the

potential suppression of A1-7-Mas-dependent pathway by ACE2 deletion.¹⁹ In addition, intraperitoneal infusion of A1-7 was shown to alleviate muscle weakness in 24-month-old ACE2 KO and wild-type (WT) mice, but not in Mas KO mice.¹⁹ These suggest that lifelong attenuation of physiological Mas-A1-7 activation does not induce muscle weakness, whereas overactivation of Mas by exogenous A1-7 or pathological conditions alleviates muscle disorders, including muscle weakness, in old mice.

In contrast to the abundant insights into the contribution of Mas in skeletal muscle, there is relatively little information about the association between AT2 and skeletal muscle function. Yoshida et al reported that AT2 expression increases with regeneration of skeletal muscle after injury or differentiation of muscle progenitor cells (satellite cells).²¹ They also reported that muscle regeneration after injury in mice was accelerated and attenuated by AT2 agonist and AT2 antagonist (or siRNA of AT2), respectively.²¹ These findings highlight certain functional roles of AT2 in skeletal muscles, but the influence of AT2 on aging-associated muscle weakness remains to be determined.

In this study, we used AT2 knockout (AT2 KO) mice to investigate whether lifelong inhibition of the angiotensin II-AT2 pathway affects the aging process in mice, primarily by focusing on skeletal muscle function. In addition, we used AT2/Mas double knockout (AT2/Mas KO) mice to investigate whether dual inhibition of the protective pathways against RAS would promote different synergistic effects in the aging process in mice compared with single deletions. Through this study, we aimed to reveal the overall significance of RAS regulation in the context of modulation of muscle function during aging.

METHODS

The data that support the findings of this study are available from the corresponding author upon reasonable request.

Experimental Design

Male WT mice, AT2 KO mice,²² and AT2/Mas KO mice generated in a C57BL/6J background were used in the study. AT2/Mas KO mice were obtained from mating AT2 KO mice and Mas KO mice.²³ These mice were maintained under specific pathogen-free conditions at 22°C under a 12-hour light-dark cycle and received standard chow and water ad libitum. Grip strength and body weight were measured periodically at 6, 12, 18, and 24 months of age. At 24 months, tissues were extracted for further analysis. Mice were anesthetized with intraperitoneal injection of a mixture of medetomidine (0.75 mg/kg), midazolam (4 mg/

kg), and butorphanol (5 mg/kg) following guidelines of the Osaka University Institutional Animal Care and Committee. We prepared 7 to 9 mice in each group,

but lost several mice before the final tissue excision mostly attributable to accidental deaths (number of animals in each time point are shown in Figure 1). The

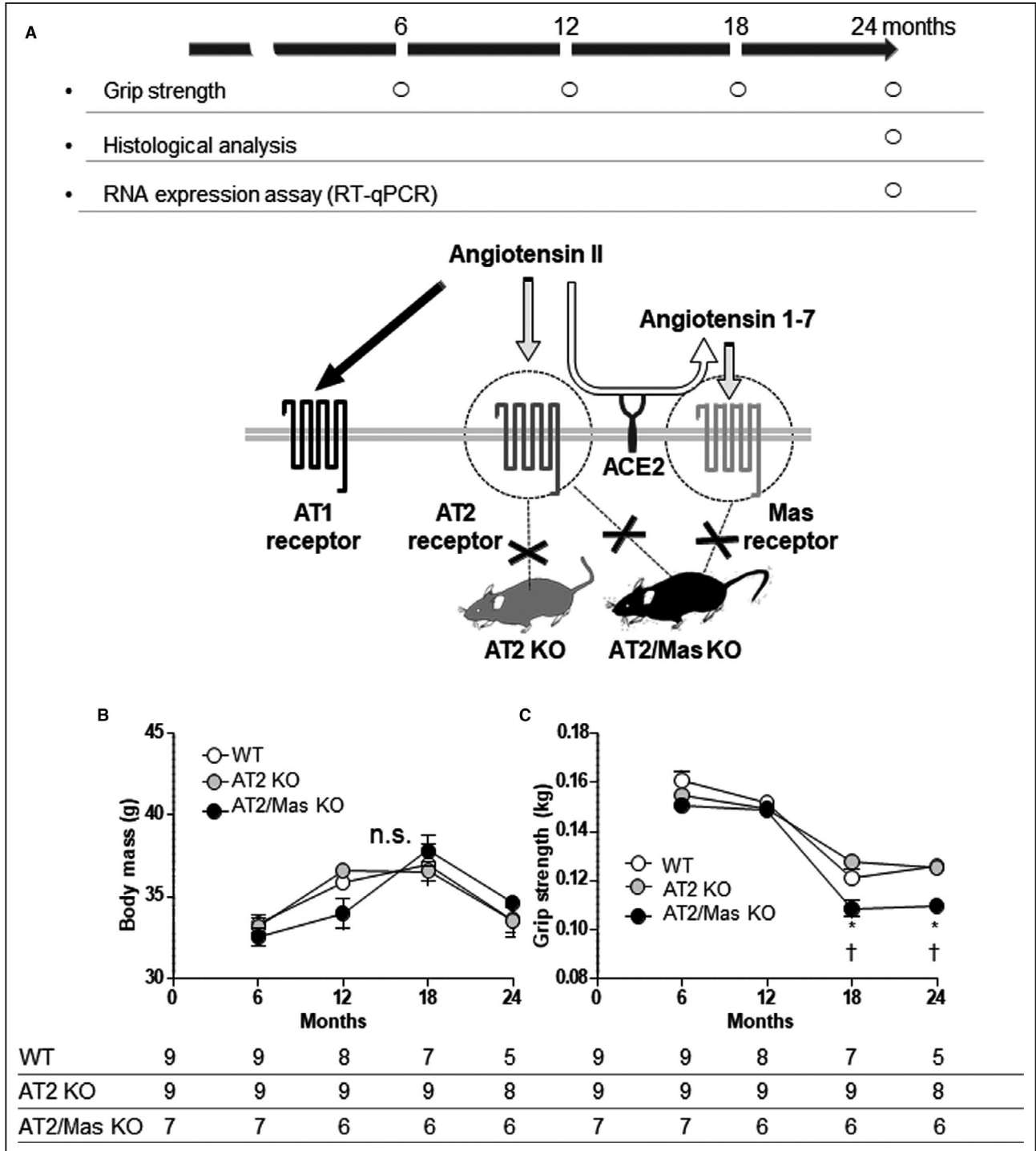


Figure 1. Schematic overview and aging-induced changes in body weight and grip strength of mice.
A, Schematic overview of the experimental protocol. Body weight (**B**) and grip strength (**C**) in mice during the experimental period. The numbers of WT, AT2 KO, and AT2/Mas KO mice were 5, 8, and 6, respectively. (Several mice died before the final excision of tissues.) Difference was analyzed with 1-way ANOVA, using a Bonferroni post hoc test. * $P < 0.05$, WT vs AT2/Mas KO. † $P < 0.05$, AT2 KO vs AT2/Mas KO. ACE2 indicates angiotensin-converting enzyme 2; AT1, angiotensin II type 1 receptor; AT2, angiotensin II type 2 receptor; AT2 KO, AT2 knockout; AT2/Mas KO, AT2/Mas double knockout; RT-qPCR, quantitative real-time polymerase chain reaction; n.s., not significant and WT, wild-type.

Animal Care and Use Committee of Osaka University and Ehime University approved the study protocol. All experiments were performed strictly according to the US National Institutes of Health *Guide for the Care and Use of Laboratory Animals*. All efforts were made to reduce animal suffering and to minimize the number of animals used.

Estimation of Grip Strength

Grip strength was measured on a digital force transducer (GPM-100; Melquest, Toyama, Japan), as previously described.²⁴ We performed 6 consecutive measurements a day for 3 days. The first day was allotted for training, whereas data acquired on the second and third days were analyzed. The average of 12 measurements was used to represent grip strength for each animal. The measurements were performed by 2 investigators, and each group of mice were blinded to the investigator who performed the measurements. All test sessions were performed during the afternoon hours of the light cycle (11 AM to 5 PM) in the vivarium where the animals were housed.

RNA Extraction and Quantitative Real-Time Polymerase Chain Reaction

Total RNA was extracted from mouse tissues using Sepasol (R)-RNA Super G (Nacalai Tesque, Kyoto, Japan). cDNA was synthesized using a ReverTra Ace quantitative real-time polymerase chain reaction kit (FSQ-101; Toyobo, Osaka, Japan) according to the manufacturer's instructions. We performed quantitative estimation of the genes associated with RAS (*AT1*, *AT2*, *Mas*, *Renin*, *Angiotensinogen*, *ACE*, and *ACE2*), the proinflammatory senescence-associated secretory phenotype (*p16*, *p19*, *p21*, *p53*, *PAI-1*, *IGFBP2*, *MMP13*, *IL-6*, *TNF- α* , and *MCP-1*),²⁵⁻²⁷ muscle-specific gene markers of senescence (*MuRF-1*, *Atrogin-1*, and *Myostatin*),^{28,29} mitochondrial function (*Mfn1*, *Mfn2*, and *DRP1*), and fibrosis (α -SMA, *TGF- β 1*, *COL1A1*, and *CTGF*), relative to *GAPDH* expression in the vastus muscle. Quantitative real-time polymerase chain reaction was performed with the SYBR Green qPCR system (Takara, Shiga, Japan) and a 7900HT Fast Real-Time PCR instrument (Applied Biosystems, Chiba, Japan). Data were analyzed with SDS software 2.4 (Applied Biosystems). Relative expression was calculated using the $\Delta\Delta C_t$ method, with data normalized using *GAPDH* as an internal control. The primer pairs used in the study are listed in Table S1.

Histological and Morphological Analysis

For hematoxylin and eosin (H&E) and Masson's trichrome staining, skeletal muscles were fixed using 4% paraformaldehyde for 24 hours after excision. The samples were then dehydrated using an alcohol

gradient and embedded in paraffin. Thereafter, the samples were sectioned at 10- μ m thickness and deparaffinized in xylene, rehydrated, and stained with H&E and Masson's trichrome according to conventional methods. For succinate dehydrogenase (SDH) staining, the vastus muscles were immediately frozen after excision in liquid nitrogen-cooled isopentane, covered in embedding agent (Tissue-Tek optimal cutting temperature compound; Sakura Finetek, Torrance, CA) and stored at -80°C until cryosectioning at 10- μ m thickness. All sections for analysis were collected from the midabdomen of skeletal muscles. Single muscle fiber cross-sectional area was measured in 200 myofibers from skeletal muscle in H&E-stained samples. The number of muscle fibers was estimated by dividing the area of skeletal muscle by the cross-sectional area of a single fiber of the same muscle in each mouse. The frequency of the central nucleus was analyzed by counting 1200 to 1800 myofibers from skeletal muscle in H&E-stained samples, as previously reported.³⁰ The amount of leukocyte infiltration was obtained by counting intramyofiber and interstitial leucocytes, as previously reported.³¹ The values were expressed as a percentage of the estimated number of muscle fibers.³² The percentage of area with fibrosis and number of vessels were analyzed in samples stained with Masson's trichrome. The number of vessels was evaluated by counting blood vessels having a diameter of ≥ 25 μ m in the vastus muscle and dividing the count by the area of the same muscle. SDH intensity was measured in 225 to 253 myofibers using the SDH-stained vastus muscle samples. Images of all stained and sectioned muscle fibers were acquired under a microscope (Keyence BZ-X900; Keyence, Osaka, Japan) at 20 \times magnification. Cross-sectional area and frequency of CNFs and SDH intensity were calculated using ImageJ software (version 1.51; National Institutes of Health, Bethesda, MD). The number of myofibers, area of fibrosis, and number of vessels were estimated using the BZ-X software (BZ-X version 1.4.01; Keyence).

For skin analysis, skin sections were cut perpendicular to the skin surface. These sections were permeabilized in 4% paraformaldehyde for 24 hours after excision. The samples were then dehydrated using an alcohol gradient and embedded in paraffin. Thereafter, the samples were sectioned and deparaffinized in xylene, rehydrated, and stained with H&E. The thickness of the dermis, epidermis, and fat layers was assessed using 30 to 50 random measurements on the skin surface in the vertical direction, following a previous report.³³

Measurement of Muscle Angiotensin II Content

Gastrocnemius muscles were collected into tubes and immediately frozen in liquid nitrogen and stored

at -80°C until measurement. Samples were homogenized in saline and complete protease inhibitor cocktail tablets (11697498001; Roche Applied Science, Penzberg, Germany) using TissueLyser LT (Qiagen, Hilden, Germany) with zirconia balls. Protein concentration of the homogenate was determined by Bradford protein assay (Bio-Rad Laboratories, Hercules, CA). Angiotensin II concentration in the homogenate were measured using an ELISA system (catalog number ADI-900-204; Enzo Clinical Labs, Farmingdale, NY) according to the manufacturer's instructions. Muscle angiotensin II content was calculated by angiotensin II concentration divided by protein concentration (picograms per milligram protein).

Statistical Analysis

All statistical analyses were conducted with GraphPad Prism version 5.0 (GraphPad Software, La Jolla, CA). Values are shown as mean \pm SEM or as a percentage. Statistical differences among 3 groups or between 2 groups were analyzed using 1-way ANOVA with the Bonferroni post hoc test or the Student *t* test, respectively. A value of $P < 0.05$ was considered statistically significant.

RESULTS

AT2/Mas KO Mice, But Not AT2 KO Mice, Showed Aging-Induced Reduction in Grip Strength Compared With WT Mice

We measured body weight and grip strength of WT, AT2 KO, and AT2/Mas KO mice until 24 months of age (Figure 1A). There was no difference in body weight

among the 3 types of mice during the period of data acquisition (Figure 1B). AT2 KO mice showed grip strength equivalent to that of WT mice (Figure 1C). In contrast, AT2/Mas KO mice exhibited lower grip strength than that of WT and AT2 KO mice from 18 months of age (Figure 1C).

Aging-Induced Decrease in Skeletal Muscle Weight in AT2/Mas KO Mice, But Not in AT2 KO Mice

The absolute or body mass-adjusted wet weight of internal organs, including several types of skeletal muscles, collected from 24-month-old mice are shown in Tables 1 and 2. Among skeletal muscles, the soleus muscle was lighter in AT2/Mas KO mice compared with WT, and the vastus muscle was lighter in AT2/Mas KO mice compared with both WT and AT2 KO mice. Among the other organs, we found differences in weight of only the liver, which was lighter in AT2/Mas KO mice compared with WT ones.

Morphologically Distinct Skeletal Muscles in AT2/Mas KO Mice Compared With AT2 KO Mice

Figures 2 and 3 show histological analysis of the vastus muscle in 24-month-old mice. We found that the cross-sectional area of myofibers was smaller in AT2 KO mice compared with both WT and AT2/Mas KO mice (Figure 2B). In contrast, the number of muscle fibers in AT2/Mas KO mice was fewer than that in AT2 KO mice (Figure 2C). CNFs, which are known to increase with aging in skeletal muscles,^{34,35} were more frequently observed in AT2/Mas KO mice than in AT2

Table 1. Absolute Wet Weight of Organs

	WT, n=5	AT2 KO, n=8	AT2/Mas KO, n=6
Body weight, g	33.6 \pm 0.75	33.5 \pm 0.98	34.67 \pm 4.85
Skeletal muscles, mg			
Triceps	116.03 \pm 7.64	106.43 \pm 3.73	109.48 \pm 15.32
Tibialis anterior	45.62 \pm 0.65	43.21 \pm 1.48	42.6 \pm 5.99
Gastrocnemius	128.52 \pm 5.21	135.56 \pm 5.48	128.7 \pm 18.45
Soleus	9.44 \pm 1.5	7.76 \pm 0.44	5.17 \pm 1.07*
Extensor digitorum longus	7.24 \pm 0.74	7.70 \pm 0.62	7.97 \pm 1.09
Rectus femoris	88.06 \pm 3.85	79.16 \pm 3.34	83.48 \pm 11.93
Vastus	98.2 \pm 5.75	92.9 \pm 6.46	69.27 \pm 12.2*
Organs, mg			
Heart	163.22 \pm 6.1	151.93 \pm 3.96	163.6 \pm 23.16
Kidney, average	231.52 \pm 10.41	223.78 \pm 10.53	224.18 \pm 30.88
Adipose tissue	335.56 \pm 36.35	385.38 \pm 49.86	287.88 \pm 55.53
Liver	1729.1 \pm 92.25	1553.08 \pm 60.71	1501.33 \pm 216.73
Spleen	99.84 \pm 13.26	95.54 \pm 8.34	84.73 \pm 16.03

Differences were analyzed by a 1-way ANOVA using the Bonferroni post hoc test. AT2 indicates angiotensin II type 2 receptor; AT2 KO, AT2 knockout; AT2/Mas KO, AT2/Mas double knockout; and WT, wild-type.

* $P < 0.05$ vs WT.

Table 2. Body Mass–Adjusted Wet Weight of Organs

	WT, n=5	AT2 KO, n=8	AT2/Mas KO, n=6
Skeletal muscles, mg			
Triceps	3.47±0.26	3.18±0.09	3.16±0.45
Tibialis anterior	1.36±0.04	1.29±0.04	1.23±0.17
Gastrocnemius	3.83±0.17	4.04±0.08	3.71±0.55
Soleus	0.28±0.04	0.23±0.01	0.15±0.03*
Extensor digitorum longus	0.22±0.02	0.23±0.02	0.23±0.03
Rectus femoris	2.63±0.16	2.36±0.07	2.41±0.35
Vastus	2.93±0.21	2.76±0.14	2.00±0.37*†
Organs, mg			
Heart	4.86±0.14	4.55±0.11	4.72±0.67
Kidney, average	6.89±0.25	6.66±0.19	6.47±0.91
Adipose tissue	9.99±1.11	11.31±1.26	8.24±1.57
Liver	51.37±1.97	46.46±1.68	43.31±6.30*
Spleen	2.99±0.43	2.78±0.20	2.45±0.47

Differences were analyzed by a 1-way ANOVA using the Bonferroni post hoc test. AT2 indicates angiotensin II type 2 receptor; AT2 KO, AT2 knockout; AT2/Mas KO, AT2/Mas double knockout; and WT, wild-type.

* $P < 0.05$ vs WT.

† $P < 0.05$ vs AT2 KO.

KO mice (Figure 2D). These findings were consistent with those in the tibialis anterior muscle, where fewer muscle fibers and an increased number of CNFs were observed in AT2/Mas KO mice (Figure S1c and S1d). There was no difference in fibrosis area (Figure 3B) and number of vessels (Figure 3C) of the vastus muscle among the 3 types of mice. There was also no difference in leukocyte infiltration of the vastus and tibialis anterior muscles among the 3 types of mice (Figure 2E, Figure S1e). We also compared the histological findings of the vastus and tibialis anterior muscles between 3- and 24-month-old WT mice (Figures S2 through S4). We found that fiber size was smaller in the tibialis anterior muscle, leukocyte infiltration was larger in the vastus muscle, and frequency of CNFs was higher in the 2 types of muscles of 24-month-old mice than 3-month-old mice (Figures S2 and S4). We also found that fibrosis area was larger in the vastus muscle of 24-month-old mice than 3-month-old mice (Figure S3). Although we previously reported aging-induced thinning of subcutaneous fat in ACE2 KO mice,¹⁹ this was not observed in the AT2/Mas KO mice used in the present study (Figure S5).

Upregulation of Genes Associated With RAS Activation and Increased Angiotensin II Content in the Skeletal Muscles of AT2/Mas KO Mice, But Not in AT2 KO Mice

Using quantitative real-time polymerase chain reaction, we confirmed the deletion of *AT2* and *AT2/Mas*

in 3 different skeletal muscles, liver, heart, and adipose tissue collected from AT2 KO and AT2/Mas KO mice, respectively (Figures S6 and S7). The relative abundance of genes associated with RAS in each organ of WT mice is shown in Figure S8. In Figure 4A, we show an increase in the levels of *AT1*, *Renin*, and *ACE* (genes associated with RAS activation) in the vastus muscle of AT2/Mas KO mice compared with WT mice. This alteration in gene expression was also observed to a degree in the tibialis anterior muscle, gastrocnemius muscle, and heart, but not in adipose tissue or the liver (Figures S6a and S7a). Additionally, analysis of the gastrocnemius muscle showed an increase in tissue angiotensin II content in AT2/Mas KO mice compared with WT mice (Figure 5). There was no alteration in the genes associated with RAS and tissue angiotensin II content in muscles of AT2 KO compared with WT mice. We found no significant difference in the expression of RAS-associated genes, including *AT2* and *Mas*, in the tibialis anterior muscle between 3- and 24-month-old WT mice (Figure S9).

Genes Associated With Aging, Inflammation, and Fibrosis Showed Aging-Induced Increase in Skeletal Muscles of AT2/Mas KO Mice, But Not in AT2 KO Mice

We then investigated genes related to senescence, inflammation, and fibrosis. Among gene markers associated with cell cycle arrest and senescence (*p16*, *p19*, *p21*, and *p53*), those encoded in the same locus (*p16* and *p19*) increased in the vastus muscle in AT2/Mas KO mice, but not in AT2 KO mice (Figure 4B). Among genes associated with the proinflammatory senescence-associated secretory phenotype (*PAI-1*, *IGFBP2*, *MMP13*, *IL-6*, *TNF- α* , and *MCP-1*), *IL-6* and *MCP-1* expression increased in AT2/Mas KO mice but not in AT2 KO mice (Figure 4B). The expression of *TGF- β 1* and *COL1A1* increased in AT2/Mas KO mice among genes associated with fibrosis (α -SMA, *COL1A1*, *TGF- β 1*, and *CTGF*) (Figure 4C). As to genes associated with mitochondrial function (*Mfn1*, *Mfn2*, and *DRP1*), *Mfn2*, a regulatory factor for mitochondrial fusion, was downregulated in AT2/Mas KO mice. Changes in the expression of these genes were similarly observed in the tibialis anterior and gastrocnemius muscle, but not in heart, liver, and adipose tissues of AT2/Mas KO mice (Figures S6b, S6c, and S7b). We found no difference in SDH activity of the vastus muscle that reflects mitochondrial accumulation and activity among the 3 types of mice (Figure S10). Although there were no changes in muscle-specific signatures of aging-associated genes (*Myostatin*, *MurF-1*, and *Atrogin-1*) in the

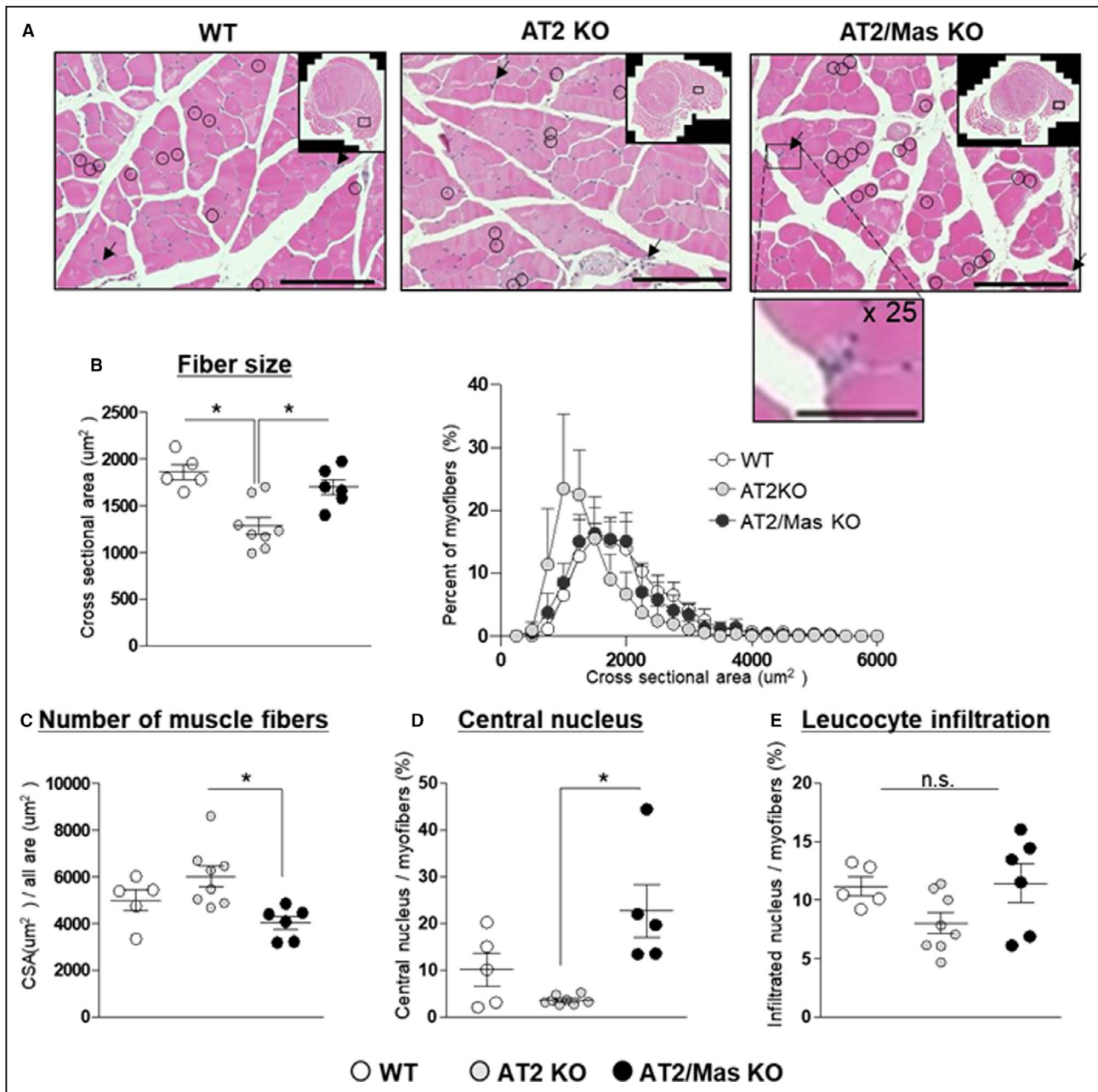


Figure 2. Histological analysis of the vastus muscle in mice.

A, Hematoxylin and eosin (H&E)-stained sections. Representative H&E-stained sections of the vastus muscle in each group of mice. **B**, Average value and distribution of cross-sectional area (CSA). The frequency of skeletal muscles was adjusted as a percentage of the total number of fibers and displayed as a histogram. **C**, Approximate number of muscle fibers in the vastus muscle, as estimated by dividing the muscle area by the CSA of a single muscle fiber in each mouse. **D**, Central nucleated fibers expressed as a percentage of total myofibers. **E**, Leucocyte infiltration determined as infiltrated nucleus expressed as a percentage of myofibers. * $P < 0.05$. AT2 indicates angiotensin II type 2 receptor; AT2 KO, AT2 knockout; AT2/Mas KO, AT2/Mas double knockout; n.s., not significant; and WT, wild-type.

vastus muscle (Figure 4C), *Myostatin* and *Atrogin-1* increased in the tibialis anterior muscle of AT2/Mas KO mice compared with AT2 KO mice, and *Myostatin* increased in the gastrocnemius muscle of AT2/Mas KO mice compared with WT and AT2 KO mice (Figure S6c).

DISCUSSION

We found that the double deletion of AT2 and Mas, but not deletion of only AT2, could substantially modify aging-associated muscle weakness in mice. Together with our previous finding that single deletion of Mas did

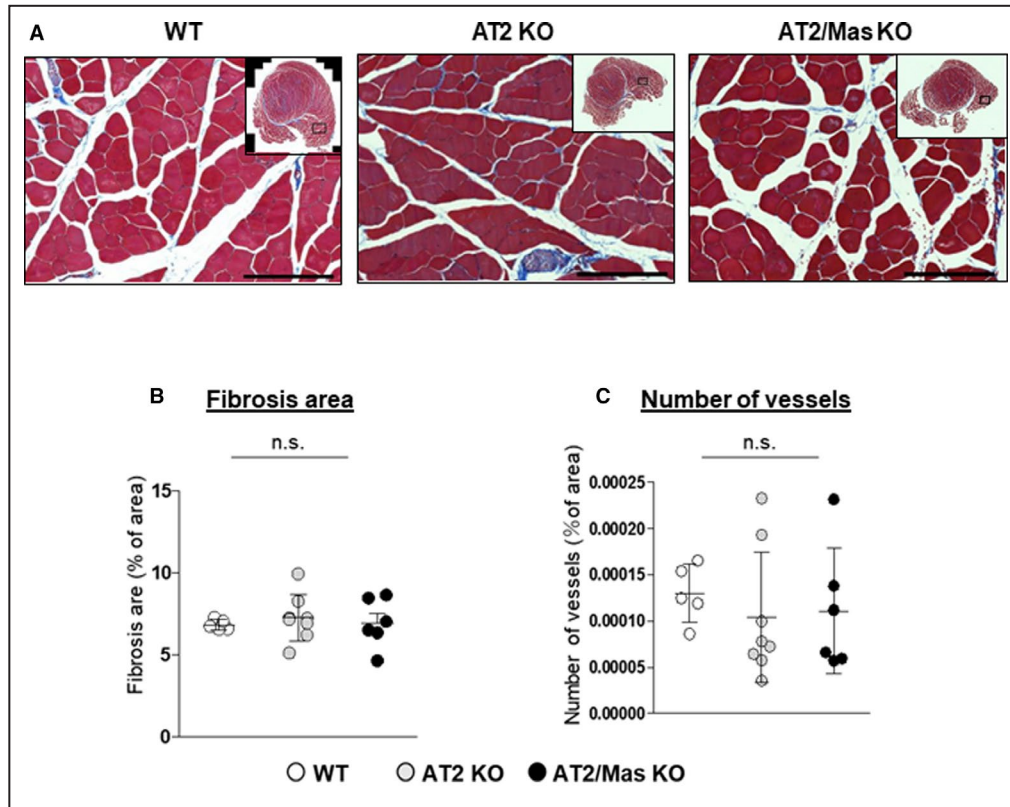


Figure 3. Histological analysis of the vastus muscle in mice.

A, Masson's trichrome–stained sections. Representative Masson's trichrome–stained sections of the vastus muscle in each group of mice. Percentage of fibrosis area (**B**) and number of vessels (**C**) in muscle fibers. Differences were analyzed with 1-way ANOVA using a Bonferroni post hoc test. Circles indicate the centrally located nuclei. Arrows indicate the infiltrated leucocytes. Scale bars: 200 μ m. AT2 indicates angiotensin II type 2 receptor; AT2 KO, AT2 knockout; AT2/Mas KO, AT2/Mas double knockout; n.s., not significant; and WT, wild-type.

not influence muscle aging in mice, this indicates that the 2 receptors involved in RAS counter-regulation are not essential by themselves, but protect skeletal muscles from advanced senescence in a complementary manner. Gene expression analysis revealed that skeletal muscles were more prominently affected by the absence of the 2 receptors compared with heart, liver, and adipose tissue. Together with the previous finding that AT2/Mas KO mice exhibit normal blood pressure,³⁶ it is conceivable that muscle, but not systemic, expression of these receptors is primarily responsible for the unique characteristics of skeletal muscles in old mice.

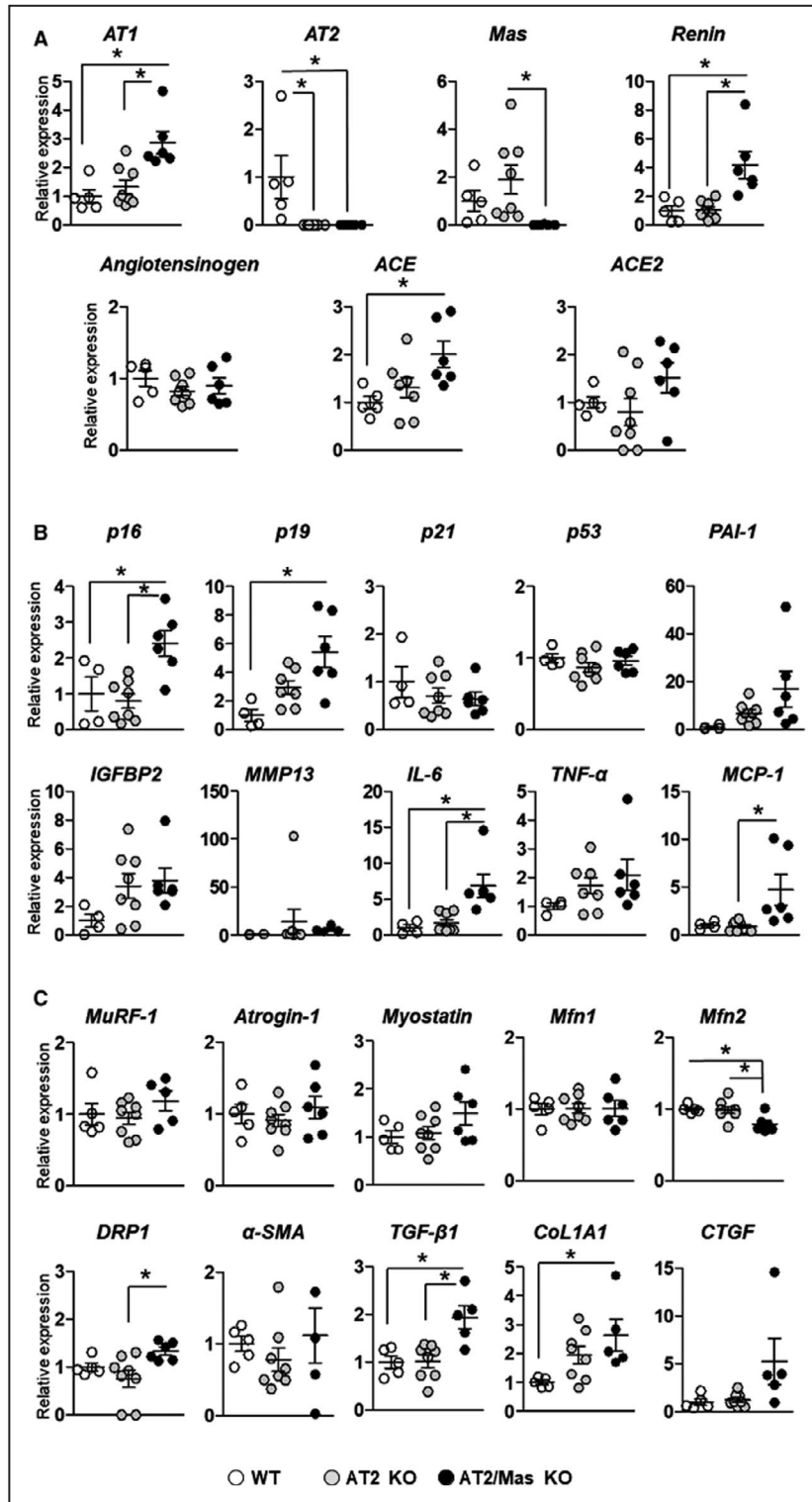
Interestingly, AT2 KO mice exhibited smaller muscle fiber size than WT and AT2/Mas KO mice, and

higher number of muscle fibers than that in AT2/Mas KO mice. In contrast, the frequency of CNFs in skeletal muscle was not altered in AT2 KO mice and increased in AT2/Mas KO mice. Although CNFs are well known to increase in regenerative processes initiated as a response to acute muscle injury, previous studies including ours have indicated that increase in CNFs is a hallmark of aging muscles.^{19,20,30,33,34} These findings suggest that although the deletion of AT2 alters muscle morphology to a certain extent, the former is not associated with accelerated aging in skeletal muscle.

In contrast to the ubiquitous expression of AT1 in adult organs, the expression of AT2 is much less abundant in adults than that in fetal tissues. In skeletal muscles, AT2 exists in muscle microvasculature³⁷ and satellite cells²¹ in

Figure 4. Quantitative real-time polymerase chain reaction analysis of age-induced changes in genes associated with the renin-angiotensin system (RAS), aging, inflammation, mitochondrial function, and fibrosis in the vastus muscle in mice.

Quantitative estimation of the expression levels of genes associated with RAS (**A**), aging and proinflammatory senescence-associated secretory phenotype (**B**), and muscle-specific gene markers of senescence, mitochondrial function, and fibrosis (**C**), relative to *GAPDH* expression in the vastus muscle. Differences were analyzed with 1-way ANOVA using the Bonferroni post hoc test. No significant difference was observed among the groups unless otherwise indicated. * $P < 0.05$. AT2 indicates angiotensin II type 2 receptor; AT2 KO, AT2 knockout; AT2/Mas KO, AT2/Mas double knockout; and WT, wild-type.



the mature stage. The expression of AT2 is upregulated in pathological conditions, such as vascular injury, myocardial infarction, congestive heart failure, and renal failure.³⁸⁻⁴¹ Likewise, AT2 was upregulated in skeletal muscles with pharmacologically or genetically induced fibrosis.⁴² The expression of Mas was also upregulated in pathological conditions, including muscle wasting, in rodents.^{43,44}

We recently reported that 18-month-old Tsukuba hypertensive mice, carrying the genes for both human renin and angiotensinogen, exhibited ~3-fold increase in the muscle expression of Mas, compared with WT mice.⁴⁵ Therefore, these receptors could be upregulated in skeletal muscles to counteract pathogenic stimuli, including RAS activation. However, these pathological conditions

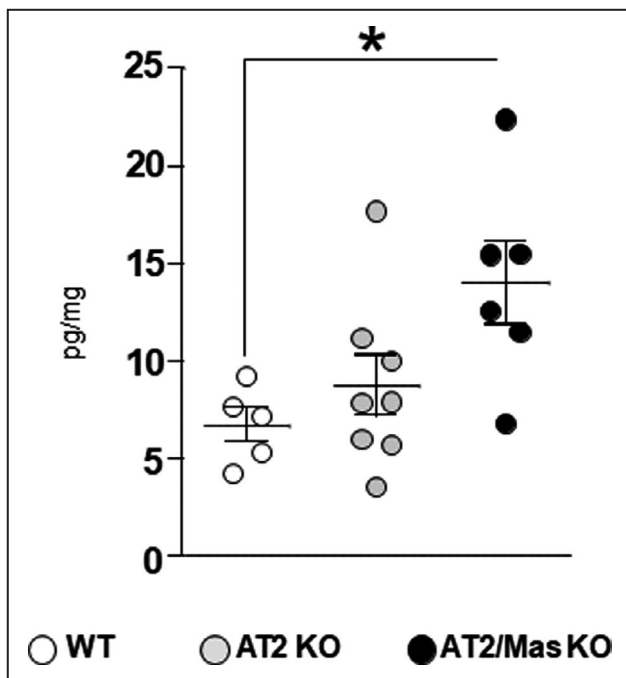


Figure 5. Angiotensin II content in the gastrocnemius muscle.

Angiotensin II content was adjusted by protein concentration of tissue lysate. Differences were analyzed with 1-way ANOVA using the Bonferroni post hoc test. * $P < 0.05$. AT2 indicates angiotensin II type 2 receptor; AT2 KO, AT2 knockout; AT2/Mas KO, AT2/Mas double knockout; and WT, wild-type.

are distinct from the physiological aging process, as investigated in the present study. We found that aging is not a transcriptional inducer of the expression of these 2 receptors, as shown in the similar expression level of the corresponding genes in 3- and 24-month-old WT mice (Figure S9). We previously found that A1-7 administration improved muscle weakness in 24-month-old mice via a Mas-dependent pathway, suggesting that the physiological expression level of this receptor is functionally relevant in skeletal muscles. In contrast, we found no aging-related changes in muscle function in Mas KO mice. This led us to conclude that a physiological level of A1-7 is not associated with the maintenance of muscle function during aging. However, this conclusion needs to be revised, because our current findings have uncovered the substantial role of Mas in maintaining skeletal muscle homeostasis in the absence of AT2. We found that deletion of only AT2 or Mas did not alter the muscle expression of *Mas* (Figure 4A) or *AT2*,¹⁹ respectively. Therefore, the distinct characteristics in mice with the double deletion of AT2 and Mas compared with those with deletion of either gene indicate that these receptors interact functionally, but not transcriptionally, with each other in skeletal muscle cells. This conclusion may be further strengthened by a future study investigating exacerbation of the aging process in old AT2 KO mice by the Mas antagonist, A779.

Interestingly, Villela et al showed that AT2 and Mas form a heterodimer and deletion of either receptor blunted the effect of agonists for both receptors in astrocytes.⁴⁶ This physical and functional interaction of the receptors appears to be contradicted by our findings, suggesting that AT2 and Mas function independently to prevent excessive aging in muscle. However, this discrepancy may be explained by potential tissue specificity of the receptor interaction in vivo, as summarized extensively in a previous review.⁴⁶ The in vivo evidence has shown that inhibition of either Mas or AT2 can blunt the effect of both receptors in certain tissues, though the signaling pathways for Mas or AT2 were reported to be intact in vascular tissue in the absence of AT2 or Mas, respectively, suggesting that the effect of the receptor interaction varies across the tissues.⁴⁶ Conversely, our findings of muscle-specific aging phenotypes in AT2/Mas KO mice, but not in AT2 KO mice, suggest that the physical interaction between AT2 and Mas is less relevant biologically in skeletal muscle.

Importantly, genes in RAS components were up-regulated specifically in the skeletal muscles of old AT2/Mas KO mice. *AT1*, *Renin*, and *ACE* increased in 2 different skeletal muscles in 24-month-old AT2/Mas KO mice. We also found that muscle angiotensin II content increased in old AT2/Mas KO mice, suggesting that local angiotensin II production is chronically accelerated in the absence of the 2 pathways conferring protection against RAS activation. The local activation of RAS in AT2/Mas KO mice is also supported by the increase of profibrotic genes including *TGF- β 1* and *COL1A1*, whereas no obvious morphological increase in fibrosis area was observed in skeletal muscles. In particular, RAS activation is known to exert profibrotic effects via elevated expression of *TGF- β 1* in skeletal muscle cells.^{17,47} Muscle *IL-6*, whose expression increased in AT2/Mas KO mice, is also reported to be a key molecule in mediating angiotensin II-induced muscle wasting.⁴⁸ Although it remains unclear how the double deletion of AT2 and Mas up-regulated genes involved in angiotensin II biosynthesis, it is possible that the 2 receptors prevent transcriptional activation of muscle RAS, which could eventually lead to aging-induced muscle weakness, in a complementary fashion. It should be noted that these findings in skeletal muscles contrast with the findings in other tissues of AT2/Mas KO mice (including liver and adipose tissues), in which the alteration of gene expression profiles was not obvious. The relative abundance of RAS-associated genes in WT mice did not appear to explain the specific transcriptional regulation of these genes in the skeletal muscle of AT2/Mas KO mice (Figure S8). Further investigation will be required to elucidate the underlying mechanism and explain the intriguing tissue specificity of transcriptional regulation of RAS by the absence of these 2 receptors.

We recently reported that ACE2 deletion could accelerate aging phenotypes, including muscle weakness, in mice.^{19,20} However, the aging process in ACE2 KO and AT2/Mas KO mice appears to be different with respect to several aspects. In contrast to the aging-induced decrease in muscle strength in AT2/Mas KO mice, ACE2 KO mice manifested muscle weakness as early as 6 months after birth.²⁰ Old ACE2 KO mice exhibited thinning of subcutaneous fat and increased expression of *p16* in adipose tissues as well as skeletal muscles. This is also in contrast to the characteristics of aged AT2/Mas KO mice, in which the specific aging phenotype is limited to skeletal muscles and are not observed in adipose tissues. We also found that *p16*, but not profibrotic and proinflammatory genes, was up-regulated in 15-month-old ACE2 KO mice. Therefore, it is conceivable that the chronic increase of profibrotic and proinflammatory stimuli is involved in the development of accelerated muscle senescence in AT2/Mas KO mice, but not in ACE2 KO ones.²⁰ Collectively, our current findings in AT2/Mas KO mice are not likely to support the involvement of RAS in accelerated aging phenotypes in ACE2 KO mice. ACE2 has multifunctional roles besides its involvement in RAS,^{49–52} and further investigations will be required to identify the role of ACE2 responsible for the specific characteristics of ACE2 KO mice during aging.

Finally, the study limitations should be noted. First, as shown in Figure 1, we lost several mice during the observation mostly because of accidental deaths, and the decrease in the number of animals could potentially decrease the statistical power in the analysis of tissues. Thus, caution should be paid on the interpretation of certain analysis that could be interfered by type II error. Second, we did not find significant difference in muscle morphology between old WT and AT2/Mas KO mice, suggesting that muscle weakness observed in old AT2/Mas KO mice was not attributed to muscle fiber atrophy. Although it is conceivable that the double deletion of AT2 and Mas reduces the contractile capacity of single muscle fiber, this hypothesis was not confirmed because of the lack of single-fiber analysis. Third, we used only male mice in the present study because of the limited capacity of the animal facility. Therefore, a potential sex difference in the present findings remains undetermined.

CONCLUSIONS

Double deletion, but not single deletion of AT2 or Mas receptors, which are the primary receptors involved in the RAS counter-regulatory axis, was found to accelerate aging-induced muscle weakness in mice. Aged AT2/Mas KO mice exhibited gene signatures of RAS activation, accompanied by the induction of profibrotic

and proinflammatory gene expression and reduced mitochondrial dysfunction, in skeletal muscles. These findings support the pivotal and complementary role of AT2 and Mas in maintaining skeletal muscle homeostasis during aging, which prevents the local activation of RAS.

ARTICLE INFORMATION

Received January 25, 2021; accepted April 16, 2021.

Affiliations

Department of Geriatric and General Medicine, Osaka University Graduate School of Medicine, Suita, Japan (H.T., K.Y., Y.W., Y.N., T.F., S.Y., K.H., F.N., H.A., Y.T., Y.T., K.S., H.R.); Department of Pharmacology (M.M.) and Department of Molecular Cardiovascular Biology and Pharmacology, Ehime University Graduate School of Medicine, Ehime, Japan (M.H.).

Acknowledgments

The authors are most grateful to H. Kitamura for her excellent technical assistance.

Sources of Funding

This work was supported by a Grant-in-Aid for Scientific Research (No. J550703552).

Disclosures

None.

Supplementary Material

Table S1
Figures S1–S10

REFERENCES

- Cabello-Verrugio C, Morales MG, Rivera JC, Cabrera D, Simon F. Renin-angiotensin system: an old player with novel functions in skeletal muscle. *Med Res Rev*. 2015;35:437–463. DOI: 10.1002/med.21343.
- Cabello-Verrugio C, Córdova G, Salas JD. Angiotensin II: role in skeletal muscle atrophy. *Curr Protein Pept Sci*. 2012;13:560–569. DOI: 10.2174/138920312803582933.
- Cabello-Verrugio C, Rivera JC, Garcia D. Skeletal muscle wasting: new role of nonclassical renin-angiotensin system. *Curr Opin Clin Nutr Metab Care*. 2017;20:158–163. DOI: 10.1097/MCO.0000000000000361.
- Santos RAS, Sampaio WO, Alzamora AC, Motta-Santos D, Alenina N, Bader M, Campagnole-Santos MJ. The ACE2/angiotensin-(1–7)/MAS axis of the renin-angiotensin system: focus on angiotensin-(1–7). *Physiol Rev*. 2018;98:505–553. DOI: 10.1152/physrev.00023.2016.
- Powers SK, Morton AB, Hyatt H, Hinkley MJ. The renin-angiotensin system and skeletal muscle. *Exerc Sport Sci Rev*. 2018;46:205–214. DOI: 10.1249/JES.0000000000000158.
- Du Bois P, Pablo Tortola C, Lodka D, Kny M, Schmidt F, Song K, Schmidt S, Bassel-Duby R, Olson EN, Fielitz J. Angiotensin II induces skeletal muscle atrophy by activating TFEB-mediated MuRF1 expression. *Circ Res*. 2015;117:424–436. DOI: 10.1161/CIRCRESAHA.114.305393.
- Song YH, Li Y, Du J, Mitch WE, Rosenthal N, Delafontaine P. Muscle-specific expression of IGF-1 blocks angiotensin II-induced skeletal muscle wasting. *J Clin Invest*. 2005;115:451–458. DOI: 10.1172/JCI22324.
- Yoshida T, Semprun-Prieto L, Sukhanov S, Delafontaine P. IGF-1 prevents ANG II-induced skeletal muscle atrophy via Akt- and Foxo-dependent inhibition of the ubiquitin ligase atrogen-1 expression. *Am J Physiol Heart Circ Physiol*. 2010;298:H1565–H1570. DOI: 10.1152/ajpheart.00146.2010.
- Cohn RD, van Erp C, Habashi JP, Soleimani AA, Klein EC, Lisi MT, Gamradt M, ap Rhys CM, Holm TM, Loeyls BL, et al. Angiotensin II type 1 receptor blockade attenuates TGF-beta-induced failure of muscle regeneration in multiple myopathic states. *Nat Med*. 2007;13:204–210. DOI: 10.1038/nm1536.

10. Elbaz M, Yanay N, Aga-Mizrachi S, Brunschwig Z, Kassis I, Ettinger K, Barak V, Nevo Y. Losartan, a therapeutic candidate in congenital muscular dystrophy: studies in the dy2J/dy2J mouse. *Ann Neurol*. 2012;71:699–708. DOI: 10.1002/ana.22694.
11. Cabello-Verrugio C, Morales MG, Cabrera D, Vio CP, Brandan E. Angiotensin II receptor type 1 blockade decreases CTGF/CCN2-mediated damage and fibrosis in normal and dystrophic skeletal muscles. *J Cell Mol Med*. 2012;16:752–764. DOI: 10.1111/j.1582-4934.2011.01354.x.
12. Yabumoto C, Akazawa H, Yamamoto R, Yano M, Kudo-Sakamoto Y, Sumida T, Kamo T, Yagi H, Shimizu YU, Saga-Kamo A, et al. Angiotensin II receptor blockade promotes repair of skeletal muscle through down-regulation of aging-promoting C1q expression. *Sci Rep*. 2015;5:14453. DOI: 10.1038/srep14453.
13. Burks TN, Andres-Mateos E, Marx R, Mejias R, Van Erp C, Simmers JL, Walston JD, Ward CW, Cohn RD. Losartan restores skeletal muscle remodeling and protects against disuse atrophy in sarcopenia. *Sci Transl Med*. 2011;3:82ra37. DOI: 10.1126/scitranslmed.3002227.
14. Cisternas F, Morales MG, Meneses C, Simon F, Brandan E, Abrigo J, Vazquez Y, Cabello-Verrugio C. Angiotensin-(1–7) decreases skeletal muscle atrophy induced by angiotensin II through a Mas receptor-dependent mechanism. *Clin Sci*. 2015;128:307–319. DOI: 10.1042/CS20140215.
15. Jose Acuna M, Pessina P, Olguin H, Cabrera D, Vio CP, Bader M, Munoz-Canoves P, Santos RA, Cabello-Verrugio C, Brandan E. Restoration of muscle strength in dystrophic muscle by angiotensin-1-7 through inhibition of TGF-beta signalling. *Hum Mol Genet*. 2014;23:1237–1249. DOI: 10.1093/hmg/ddt514.
16. Morales MG, Abrigo J, Acuna MJ, Santos RA, Bader M, Brandan E, Simon F, Olguin H, Cabrera D, Cabello-Verrugio C. Angiotensin-(1–7) attenuates disuse skeletal muscle atrophy in mice via its receptor, Mas. *Dis Mod Mech*. 2016;9:441–449. DOI: 10.1242/dmm.023390.
17. Morales MG, Abrigo J, Meneses C, Simon F, Cisternas F, Rivera JC, Vazquez Y, Cabello-Verrugio C. The Ang-(1–7)/Mas-1 axis attenuates the expression and signalling of TGF-beta 1 induced by AngII in mouse skeletal muscle. *Clin Sci (Lond)*. 2014;127:251–264. DOI: 10.1042/CS20130585.
18. Morales MG, Olguin H, Di Capua G, Brandan E, Simon F, Cabello-Verrugio C. Endotoxin-induced skeletal muscle wasting is prevented by angiotensin-(1–7) through a p38 MAPK-dependent mechanism. *Clin Sci (Lond)*. 2015;129:461–476. DOI: 10.1042/CS20140840.
19. Nozato S, Yamamoto K, Takeshita H, Nozato Y, Imaizumi Y, Fujimoto T, Yokoyama S, Nagasawa M, Takeda M, Hongyo K, et al. Angiotensin 1–7 alleviates aging-associated muscle weakness and bone loss, but is not associated with accelerated aging in ACE2-knockout mice. *Clin Sci (Lond)*. 2019;133:2005–2018. DOI: 10.1042/CS20190573.
20. Takeshita H, Yamamoto K, Nozato S, Takeda M, Fukada S-I, Inagaki T, Tsuchimochi H, Shirai M, Nozato Y, Fujimoto T, et al. Angiotensin-converting enzyme 2 deficiency accelerates and angiotensin 1–7 restores age-related muscle weakness in mice. *J Cachexia Sarcopenia Muscle*. 2018;9:975–986. DOI: 10.1002/jcsm.12334.
21. Yoshida T, Huq TS, Delafontaine P. Angiotensin type 2 receptor signaling in satellite cells potentiates skeletal muscle regeneration. *J Biol Chem*. 2014;289:26239–26248. DOI: 10.1074/jbc.M114.585521.
22. Hein L, Barsh GS, Pratt RE, Dzau VJ, Kobilka BK. Behavioral and cardiovascular effects of disrupting the angiotensin-II type-2 receptor gene in mice. *Nature*. 1995;377:744–747.
23. Ohshima K, Mogi M, Nakaoka H, Iwanami J, Min L-J, Kanno H, Tsukuda K, Chisaka T, Bai H-Y, Wang X-L, et al. Possible role of angiotensin-converting enzyme 2 and activation of angiotensin II type 2 receptor by angiotensin-(1–7) in improvement of vascular remodeling by angiotensin II type 1 receptor blockade. *Hypertension*. 2014;63:e53–e59. DOI: 10.1161/HYPERTENSIONAHA.113.02426.
24. Takeshita H, Yamamoto K, Nozato S, Inagaki T, Tsuchimochi H, Shirai M, Yamamoto R, Imaizumi Y, Hongyo K, Yokoyama S, et al. Modified forelimb grip strength test detects aging-associated physiological decline in skeletal muscle function in male mice. *Sci Rep*. 2017;7:42323. DOI: 10.1038/srep42323.
25. Baker DJ, Weaver RL, van Deursen JM. p21 both attenuates and drives senescence and aging in BubR1 progeroid mice. *Cell Rep*. 2013;3:1164–1174. DOI: 10.1016/j.celrep.2013.03.028.
26. Edwards MG, Anderson RM, Yuan M, Kendzierski CM, Weindruch R, Prolla TA. Gene expression profiling of aging reveals activation of a p53-mediated transcriptional program. *BMC Genomics*. 2007;8:80. DOI: 10.1186/1471-2164-8-80.
27. Baker DJ, Perez-Terzic C, Jin F, Pitel KS, Niederländer NJ, Jegannathan K, Yamada S, Reyes S, Rowe L, Hiddinga HJ, et al. Opposing roles for p16(Ink4a) and p19(Arf) in senescence and ageing caused by BubR1 insufficiency. *Nat Cell Biol*. 2008;10:825–836. DOI: 10.1038/ncb1744.
28. Okumura N, Toda T, Ozawa Y, Watanabe K, Ikuta T, Tatefuji T, Hashimoto K, Shimizu T. Royal jelly delays motor functional impairment during aging in genetically heterogeneous male mice. *Nutrients*. 2018;10:1191. DOI: 10.3390/nu10091191.
29. Baumann AP, Ibejunjo C, Grasser WA, Paralkar VM. Myostatin expression in age and denervation-induced skeletal muscle atrophy. *J Musculoskelet Neuronal Interact*. 2003;3:8–16.
30. Valdez G, Tapia JC, Kang H, Clemenson GD, Gage FH, Lichtman JW, Sanes JR. Attenuation of age-related changes in mouse neuromuscular synapses by caloric restriction and exercise. *Proc Natl Acad Sci USA*. 2010;107:14863–14868. DOI: 10.1073/pnas.1002220107.
31. Yang C, Jiao Y, Wei B, Yang ZY, Wu JF, Jensen J, Jean WH, Huang CY, Kuo CH. Aged cells in human skeletal muscle after resistance exercise. *Aging*. 2018;10:1356–1365. DOI: 10.18632/aging.101472.
32. Saovieng S, Wu JF, Huang CY, Kao CL, Higgins MF, Chuanchaiyakul R, Kuo CH. Deep ocean minerals minimize eccentric exercise-induced inflammatory response of rat skeletal muscle. *Front Physiol*. 2018;9:1351. DOI: 10.3389/fphys.2018.01351.
33. Sato S, Kawamata Y, Takahashi A, Imai Y, Hanyu A, Okuma A, Takasugi M, Yamakoshi K, Sorimachi H, Kanda H, et al. Ablation of the p16(INK4a) tumour suppressor reverses ageing phenotypes of klotho mice. *Nat Commun*. 2015;6:7035. DOI: 10.1038/ncomms8035.
34. Romanick M, Thompson LV, Brown-Borg HM. Murine models of atrophy, cachexia, and sarcopenia in skeletal muscle. *Biochim Biophys Acta*. 2013;1832:1410–1420. DOI: 10.1016/j.bbdis.2013.03.011.
35. Lee ASJ, Anderson JE, Joya JE, Head SI, Pather N, Kee AJ, Gunning PW, Hardeman EC. Aged skeletal muscle retains the ability to fully regenerate functional architecture. *Bioarchitecture*. 2013;3:25–37. DOI: 10.4161/bioa.24966.
36. Higaki A, Mogi M, Iwanami J, Min L-J, Bai H-Y, Shan B-S, Kukida M, Yamauchi T, Tsukuda K, Kan-no H, et al. Beneficial effect of Mas receptor deficiency on vascular cognitive impairment in the presence of angiotensin II type 2 receptor. *J Am Heart Assoc*. 2018;7:e008121. DOI: 10.1161/JAHA.117.008121.
37. Chai W, Wang W, Liu J, Barrett EJ, Carey RM, Cao W, Liu Z. Angiotensin II type 1 and type 2 receptors regulate basal skeletal muscle microvascular volume and glucose use. *Hypertension*. 2010;55:523–530. DOI: 10.1161/HYPERTENSIONAHA.109.145409.
38. Matavelli LC, Siragy HM. AT2 receptor activities and pathophysiological implications. *J Cardiovasc Pharmacol*. 2015;65:226–232. DOI: 10.1097/FJC.0000000000000208.
39. Ruiz-Ortega M, Esteban V, Suzuki Y, Ruperez M, Mezzano S, Ardiles L, Justo P, Ortiz A, Egido J. Renal expression of angiotensin type 2 (AT2) receptors during kidney damage. *Kidney Int Suppl*. 2003;64:S21–S26. DOI: 10.1046/j.1523-1755.64.s86.5.x.
40. Levy BI. How to explain the differences between renin angiotensin system modulators. *Am J Hypertens*. 2005;18:134S–141S. DOI: 10.1016/j.amjhyper.2005.05.005.
41. Matsubara H. Pathophysiological role of angiotensin II type 2 receptor in cardiovascular and renal diseases. *Circ Res*. 1998;83:1182–1191. DOI: 10.1161/01.RES.83.12.1182.
42. Painemal P, Acuña MJ, Riquelme C, Brandan E, Cabello-Verrugio C. Transforming growth factor type beta 1 increases the expression of angiotensin II receptor type 2 by a SMAD- and p38 MAPK-dependent mechanism in skeletal muscle. *Biofactors*. 2013;39:467–475. DOI: 10.1002/biof.1087.
43. Morales MG, Abrigo J, Meneses C, Cisternas F, Simon F, Cabello-Verrugio C. Expression of the mas receptor is upregulated in skeletal muscle wasting. *Histochem Cell Biol*. 2015;143:131–141. DOI: 10.1007/s00418-014-1275-1.
44. Lu J, Jiang T, Wu L, Gao L, Wang Y, Zhou F, Zhang S, Zhang Y. The expression of angiotensin-converting enzyme 2-angiotensin-(1–7)-Mas receptor axis are upregulated after acute cerebral ischemic stroke in rats. *Neuropeptides*. 2013;47:289–295. DOI: 10.1016/j.npep.2013.09.002.
45. Takeshita H, Yamamoto K, Mogi M, Nozato S, Horiuchi M, Rakugi H. Different effects of the deletion of angiotensin converting enzyme 2 and chronic activation of the renin-angiotensin system on muscle weakness

- in middle-aged mice. *Hypertens Res.* 2019;43:296–304. DOI: 10.1038/s41440-019-0375-7.
46. Villela D, Leonhardt J, Patel N, Joseph J, Kirsch S, Hallberg A, Unger T, Bader M, Santos RA, Summers C, et al. Angiotensin type 2 receptor (AT2R) and receptor Mas: a complex liaison. *Clin Sci (Lond)*. 2015;128:227–234. DOI: 10.1042/CS20130515.
 47. Morales MG, Vazquez Y, Acuña MJ, Rivera JC, Simon F, Salas JD, Alvarez Ruf J, Brandan E, Cabello-Verrugio C. Angiotensin II-induced pro-fibrotic effects require p38MAPK activity and transforming growth factor beta 1 expression in skeletal muscle cells. *Int J Biochem Cell Biol*. 2012;44:1993–2002. DOI: 10.1016/j.biocel.2012.07.028.
 48. Zhang L, Du J, Hu Z, Han G, Delafontaine P, Garcia G, Mitch WE. IL-6 and serum amyloid A synergy mediates angiotensin II-induced muscle wasting. *J Am Soc Nephrol*. 2009;20:604–612. DOI: 10.1681/ASN.2008060628.
 49. Hashimoto T, Perlot T, Rehman A, Trichereau J, Ishiguro H, Paolino M, Sigl V, Hanada T, Hanada R, Lipinski S, et al. ACE2 links amino acid malnutrition to microbial ecology and intestinal inflammation. *Nature*. 2012;487:477–481. DOI: 10.1038/nature11228.
 50. Kuba K, Imai Y, Penninger JM. Multiple functions of angiotensin-converting enzyme 2 and its relevance in cardiovascular diseases. *Circ J*. 2013;77:301–308. DOI: 10.1253/circj.cj-12-1544.
 51. Camargo SMR, Singer D, Makrides V, Huggel K, Pos KM, Wagner CA, Kuba K, Danilczyk U, Skovby F, Kleta R, et al. Tissue-specific amino acid transporter partners ACE2 and collectrin differentially interact with hartnup mutations. *Gastroenterology*. 2009;136:872–882. DOI: 10.1053/j.gastro.2008.10.055.
 52. Sato T, Suzuki T, Watanabe H, Kadowaki A, Fukamizu A, Liu PP, Kimura A, Ito H, Penninger JM, Imai Y, et al. Apelin is a positive regulator of ACE2 in failing hearts. *J Clin Invest*. 2013;123:5203–5211. DOI: 10.1172/JCI69608.

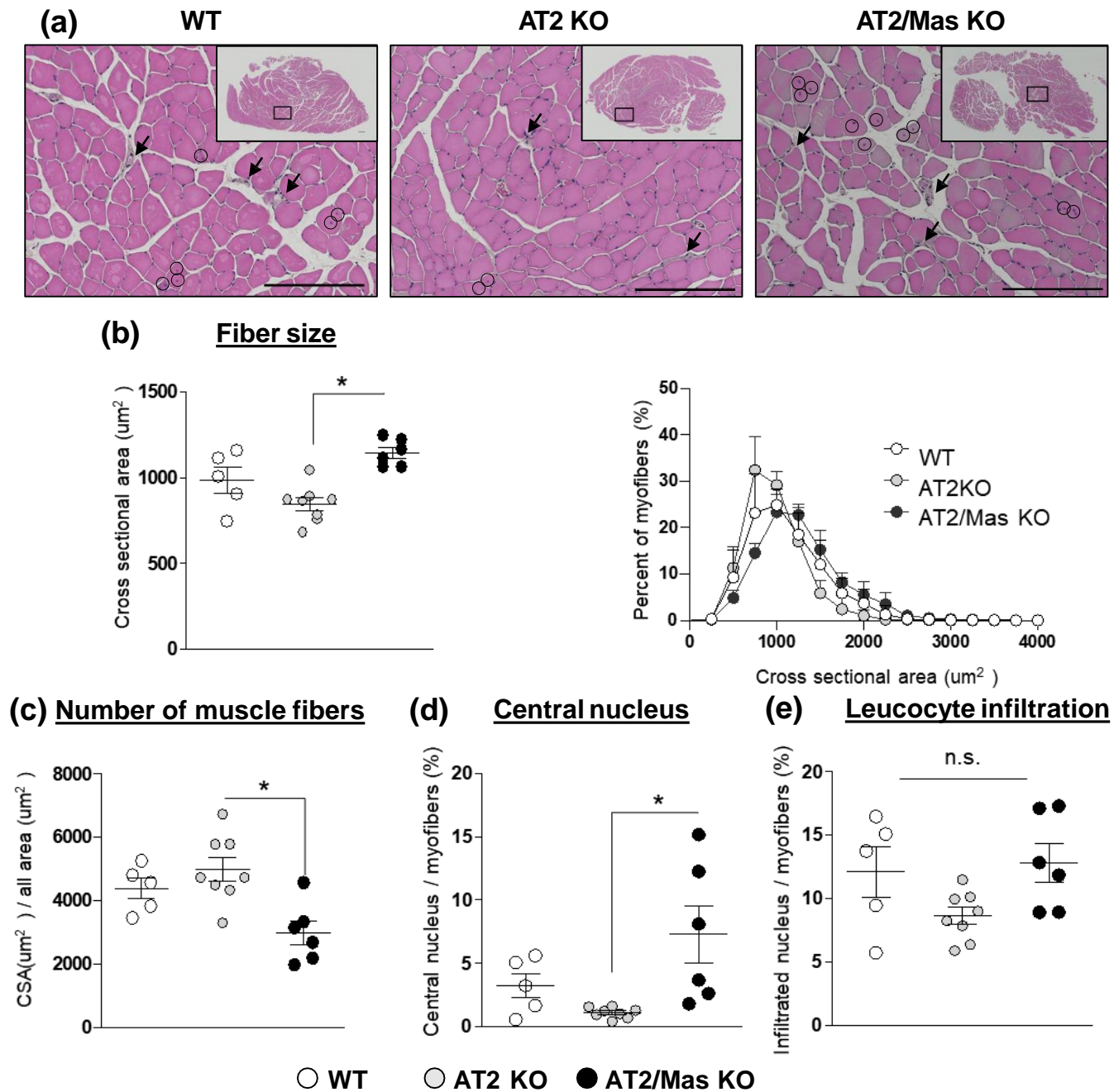
SUPPLEMENTAL MATERIAL

Table S1. Primer list

gene type	gene name	Primer Sequence	
Renin- angiotensin- system- components	<i>AT1</i>	F	TCACCTGCATCATCATCTGG
		R	AGCTGGTAAGAATGATTAGG
	<i>AT2</i>	F	CCTGCATGAGTGTCGATAGGT
		R	CCAGCAGACCACTGAGCATA
	<i>Mas</i>	F	CCTCCCATTCTTCGAAGCTGTA
		R	GCCTGGGTTGCATTTTCATCTTT
	<i>Renin</i>	F	GCCCTCTGCCACCCAGTAA
		R	CAAAGCCAGACAAAATGGCCC
	<i>Angiotensinogen</i>	F	ACCCCCGAGTGGGAGAGGTTTC
		R	GCCAGGCTGCTGGACAGACG
	<i>ACE</i>	F	TCATCATCCAGTTCCAGTTCCA
		R	CGGTGACGAGCCATTCTGT
	<i>ACE2</i>	F	CTACAGGCCCTTCAGCAAAG
		R	AATGGTGCTCATGGTGTCA
Cell cycle arrest and senescence	<i>p16</i>	F	CCGCTGCAGACAGACTGG
		R	CCATCATCATCACCTGAATCG
	<i>p19</i>	F	AAGAGAGGGTTTTCTTGGTG
		R	CATCATCATCACCTGGTCC
	<i>p21</i>	F	GACAAGAGGCCCAGTACTTCCT
		R	CAATCTGCGCTTGGAGTGATA
	<i>p53</i>	F	CCCCTGTCATCTTTTGTCCCTT
		R	GGGAGGAGAGTACGTGCACATAA

gene type	gene name	Primer Sequence		
SASP	<i>PAI-1</i>	F	TCAGAGCAACAAGTTCAACTACACTGAG	
		R	CCCCTGTCAAGGCTCCATCACTTGCCCCA	
	<i>IGFBP2</i>	F	GGGTGCCAAACACCTCAG	
		R	AGGTTGTACCGGCCATGC	
	<i>MMP13</i>	F	CTTCTACCCATTTGATGGACCTT	
		R	AAGCTCATGGGCAGCAACA	
	<i>IL-6</i>	F	CTACCCCAATTTCCAATGCT	
		R	ACCACAGTGAGGAATGTCCA	
	<i>TNF-α</i>	F	CCCTCACACTCAGATCATCTTCT	
		R	GCTACGACGTGGGCTACAG	
	<i>MCP-1</i>	F	TGTAGGTTCTGATCTCATTGG	
		R	ACTCATTACCAGCAAGATG	
	Muscle specific gene signatures of ageing	<i>MuRF-1</i>	F	GTGAAGTTGCCCCCTTACAA
			R	TGGAGATGCAATTGCTCAGT
<i>Atrogin-1</i>		F	CCATCAGGAGAAGTGGATCTATGTT	
		R	GCTTCCCCCAAAGTGCAGTA	
<i>Myostatin</i>		F	CATCTTGTGCACCAAGCAAA	
		R	GGGAGACATTTTTGTCCGAGT	
Regulatory factor for mitochondrial fusion	<i>Mfn1</i>	F	AGCCCAACATCTTCATTCTGAA	
		R	CTTACAACCTTGAGCTCTTCTACCA	
	<i>Mfn2</i>	F	CATCAGTTACACCGGCTCTAACT	
		R	GAGCCTCGACTTTCTTGTTCA	
	<i>DRP1</i>	F	GTTCCACGCCAACAGAATAC	
		R	CCTAACCCCTGAATGAAGT	

gene type	gene name	Primer Sequence	
Fibrosis	<i>αSMA</i>	F	GTCCCAGACATCAGGGAGTAA
		R	TCGGATACTTCAGCGTCAGGA
	<i>TGF-β1</i>	F	CCCCTGGAAAGGGCTCAACAC
		R	TCCAACCCAGGTCCTTCCTAAAGTC
	<i>COL1A1</i>	F	GCCGCAAAGAGTCTACA
		R	CGGGTTTCCACGTCTCA
<i>CTGF</i>	F	TCCACCCGAGTTACCAA	
	R	TTAGGTGTCCGGATGC	
House keeping gene	<i>GAPDH</i>	F	TTGTGATGGGTGTGAACCACGAGA
		R	CATGAGCCCTTCCACACAATGCCAAA
	<i>18S</i>	F	CGATCCGAGGGCCTCACTA
		R	AGTCCCTGCCCTTTGTA

Fig. S1**Histological analysis of the tibialis anterior muscle in mice.**

Representative H&E-stained sections of the tibialis anterior muscle in each group of mice (a).

Average value and distribution of CSA. The frequency of myofibers was adjusted as a percentage of the total number of fibers and displayed as a histogram (b).

Approximate number of muscle fibers in the tibialis anterior muscle, as estimated by dividing the muscle area by the CSA of a single muscle fiber in each mouse (c).

Central nucleated fibers (CNFs) expressed as a percentage of total myofibers (d).

Leucocyte infiltration determined as infiltrated nucleus expressed as a percentage of myofibers (e).

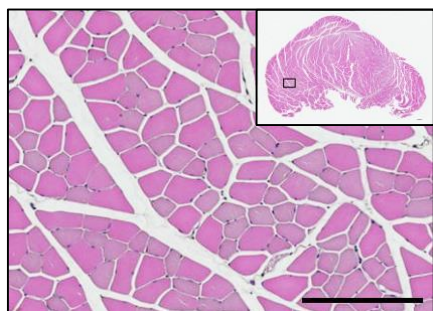
Differences were analyzed with a one-way ANOVA using a Bonferroni post-hoc test.

* $p < 0.05$; n.s., not significant

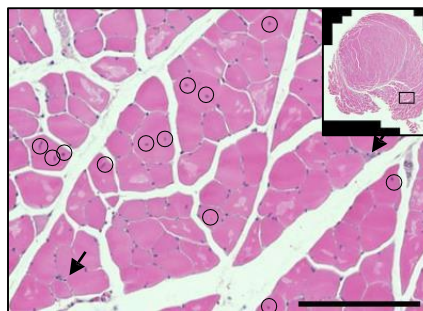
Scale bars: 200 μm . Circles indicate the centrally located nuclei. Arrows indicate the infiltrated leucocytes. WT, Wild-type.

Fig. S2

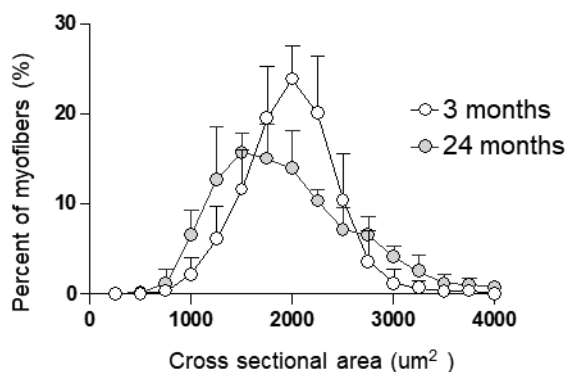
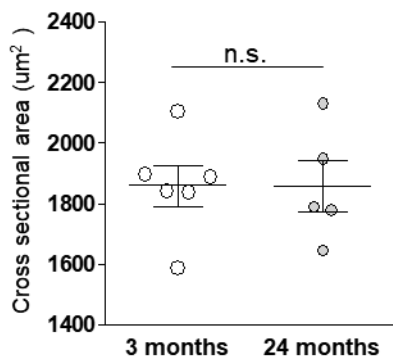
(a) 3 months



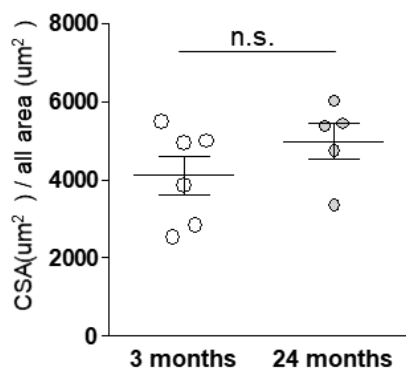
24 months



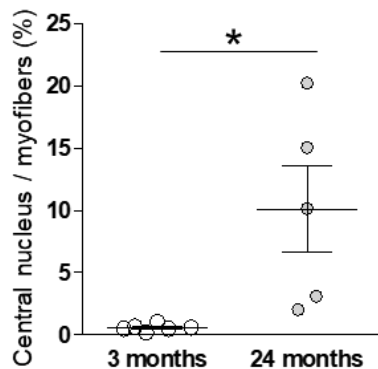
(b) Fiber size



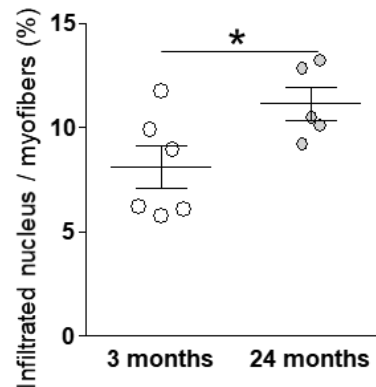
(c) Number of muscle fibers



(d) Central nucleus



(e) Leucocyte infiltration



Histological analysis of the vastus muscle in mice.

Representative H&E-stained sections of the vastus muscle in each group of mice (a).

Average value and distribution of CSA. The frequency of myofibers was adjusted as a percentage of the total number of fibers and displayed as a histogram (b).

Approximate number of muscle fibers in the vastus muscle, as estimated by dividing the muscle area by the CSA of a single muscle fiber in each mouse (c).

Central nucleated fibers (CNFs) expressed as a percentage of total myofibers (d).

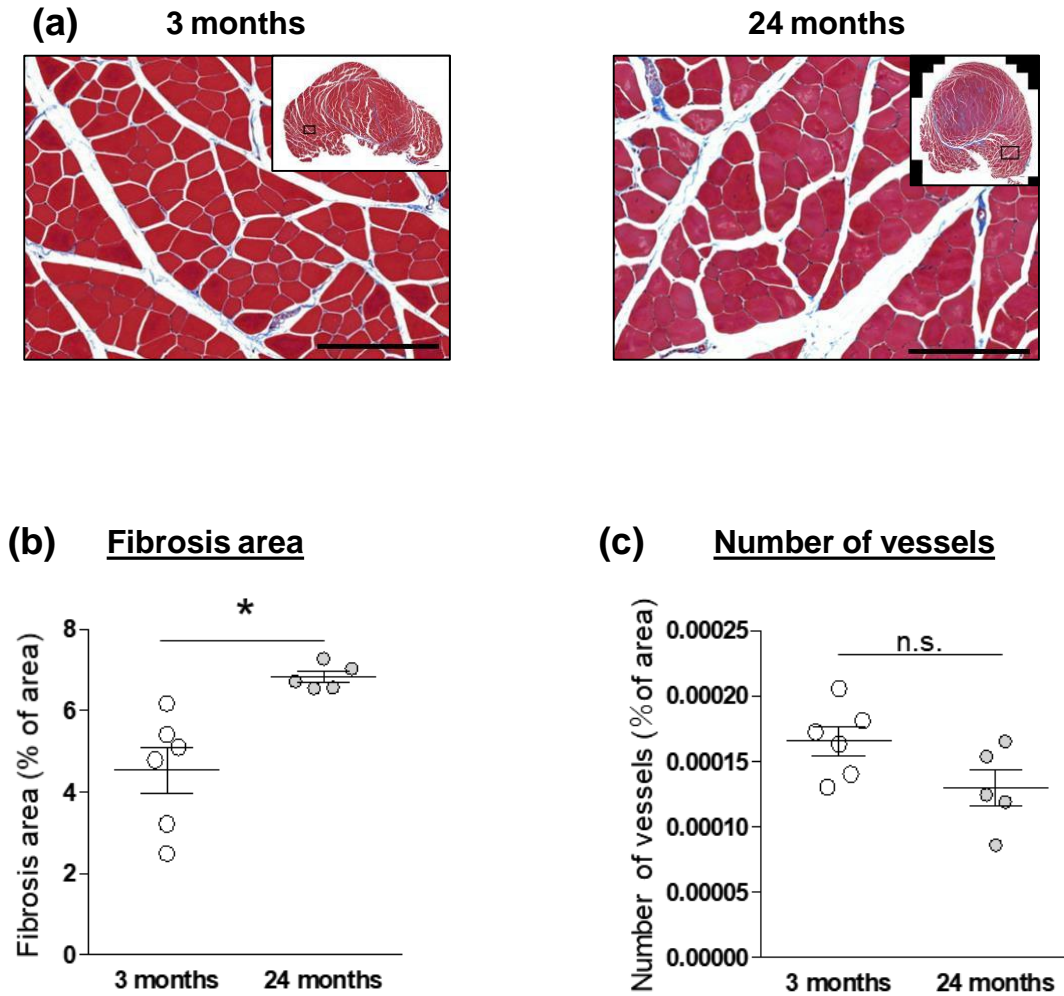
Leucocyte infiltration determined as infiltrated nucleus expressed as a percentage of myofibers (e).

Differences were analyzed with a student's t-test.

*p < 0.05; n.s., not significant

Scale bars: 200 μm. Circles indicate the centrally located nuclei. Arrows indicate the infiltrated leucocytes.

Fig. S3



Histological analysis of the vastus muscle in mice.

Representative Masson's trichrome-stained sections of the vastus muscle in each group of mice (a).

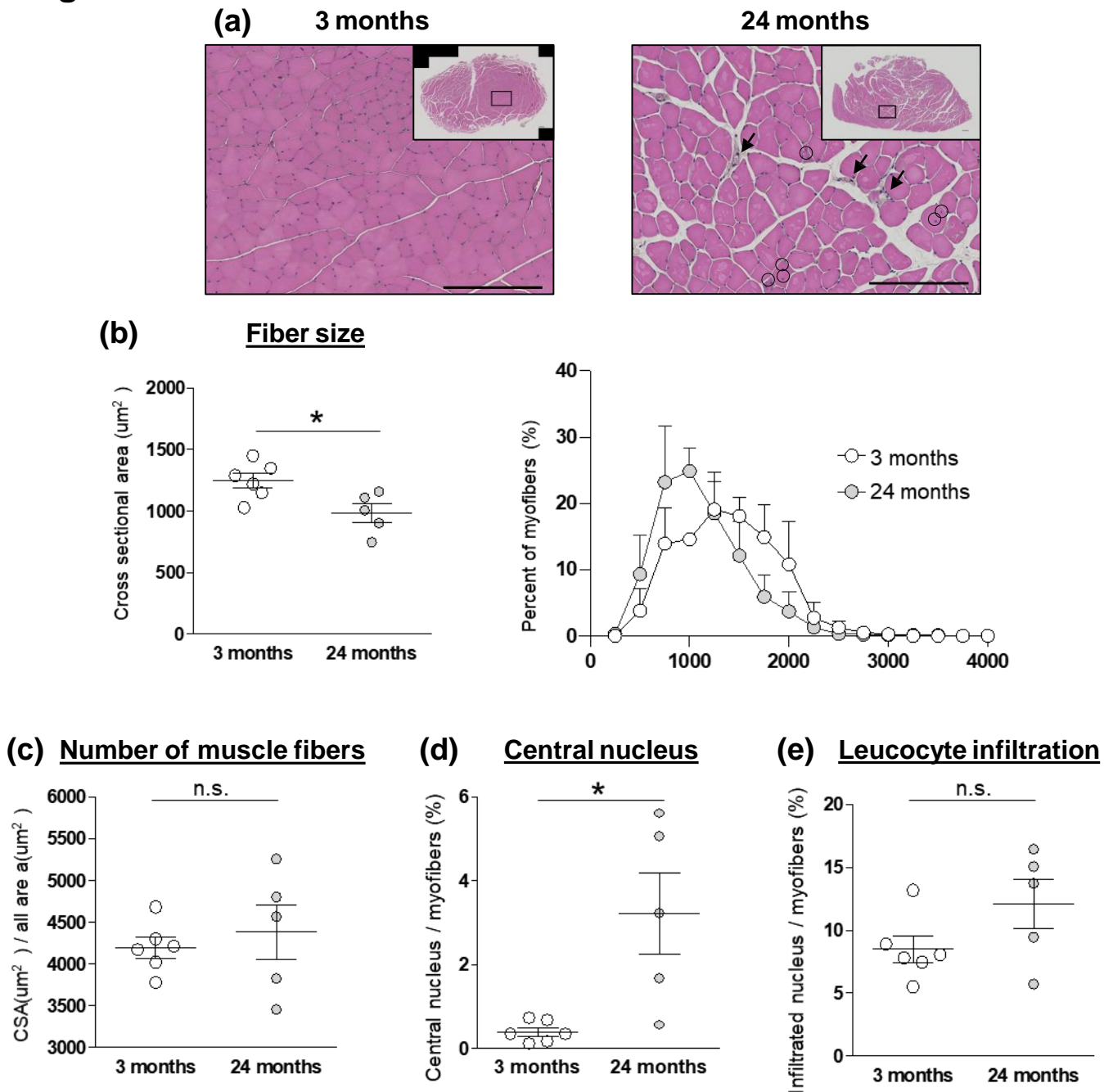
Percentage of fibrosis area (b) and number of vessels (c) in muscle fibers.

Differences were analyzed with a student's t-test.

* $p < 0.05$; n.s., not significant

Scale bars: 200 μ m.

Fig. S4



Histological analysis of the tibialis anterior muscle in mice.

Representative H&E-stained sections of the tibialis anterior muscle in each group of mice (a).

Average value and distribution of CSA. The frequency of myofibers was adjusted as a percentage of the total number of fibers and displayed as a histogram (b).

Approximate number of muscle fibers in the vastus muscle, as estimated by dividing the muscle area by the CSA of a single muscle fiber in each mouse (c).

Central nucleated fibers (CNFs) expressed as a percentage of total myofibers (d).

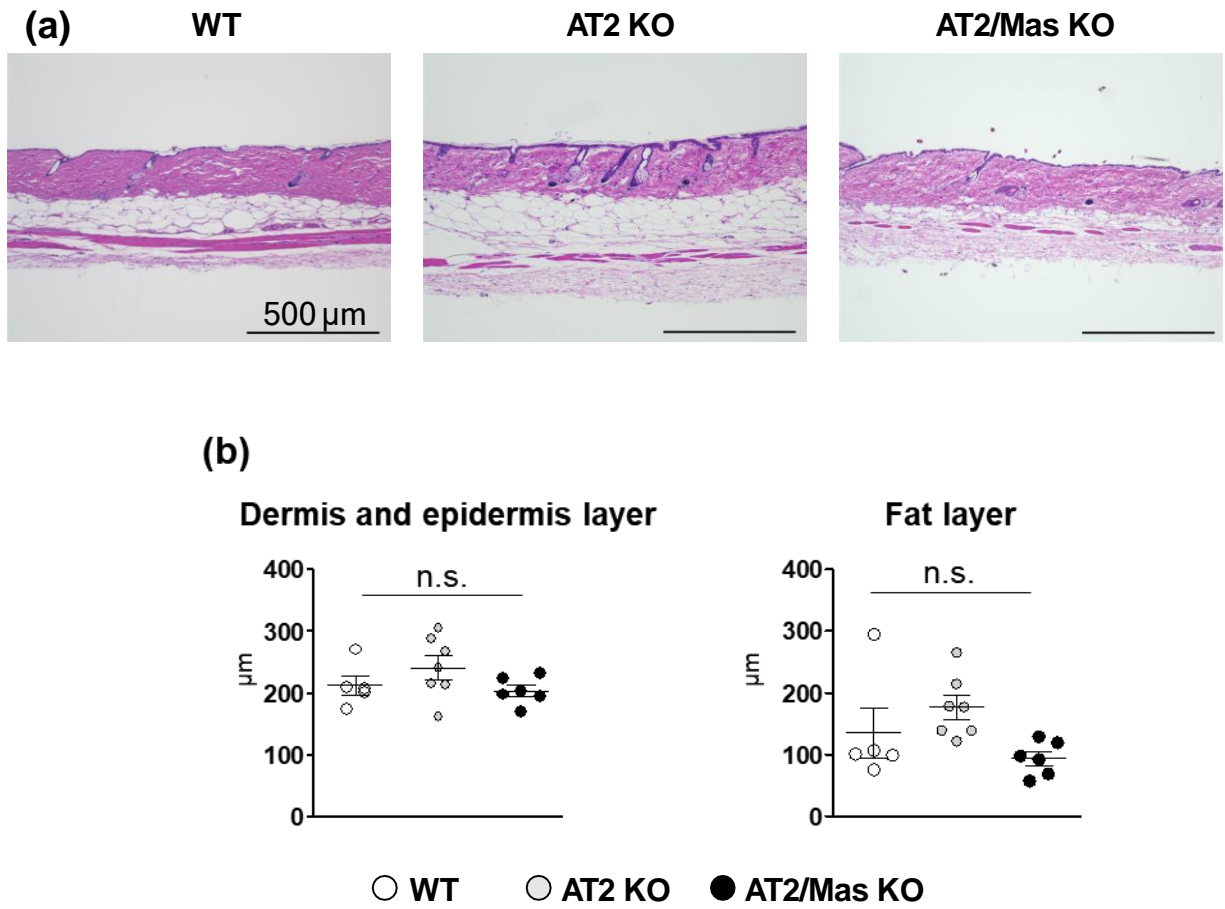
Leucocyte infiltration determined as infiltrated nucleus expressed as a percentage of myofibers (e).

Differences were analyzed with a student's t-test.

*p < 0.05; n.s., not significant

Scale bars: 200 μm. Circles indicate the centrally located nuclei. Arrows indicate the infiltrated leucocytes.

Fig. S5



Histological analysis of the skin in mice.

Representative skin sections visualized by H&E staining (a).

Quantification of thickness in dermis and epidermis layers (b) and fat layers (c).

Differences were analyzed with a one-way ANOVA using a Bonferroni post-hoc test.

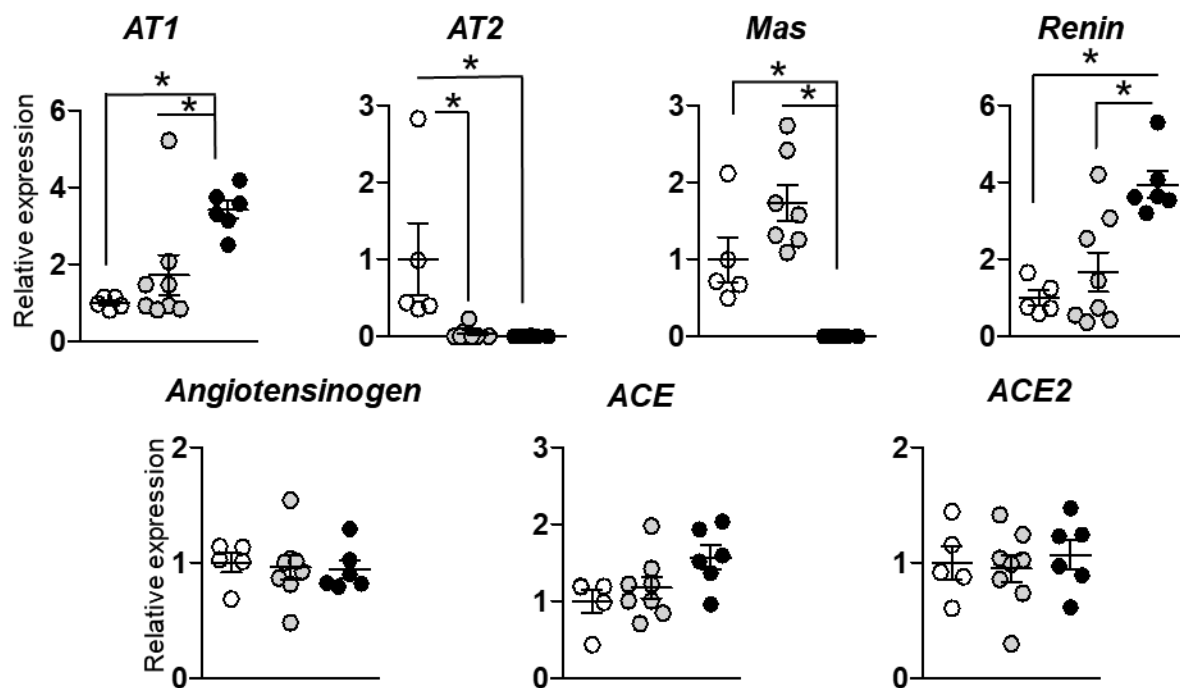
n.s., not significant

WT, Wild-type; KO, knockout

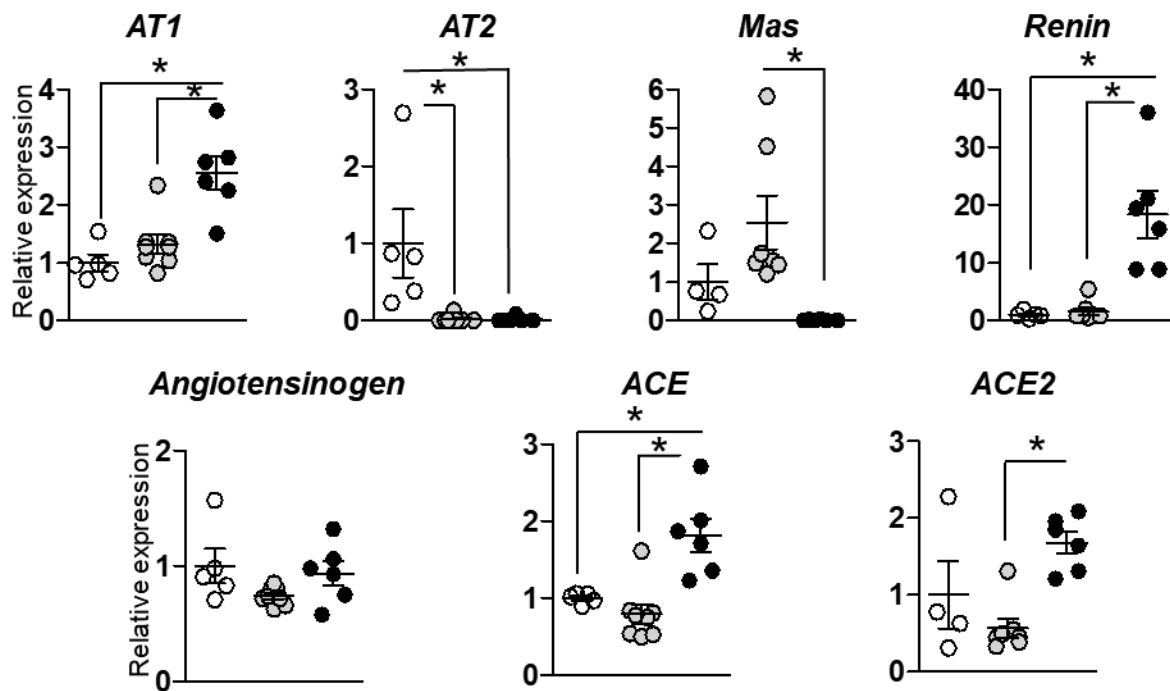
Fig. S6

(a)

Tibialis anterior muscle



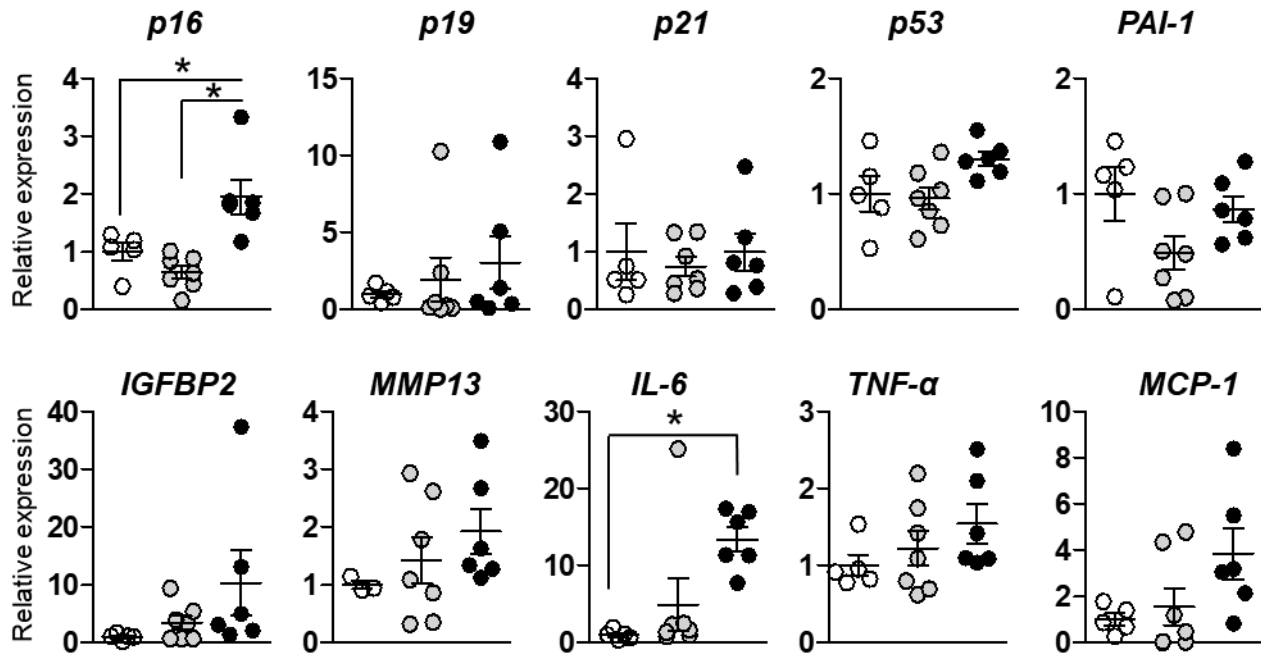
Gastrocnemius muscle



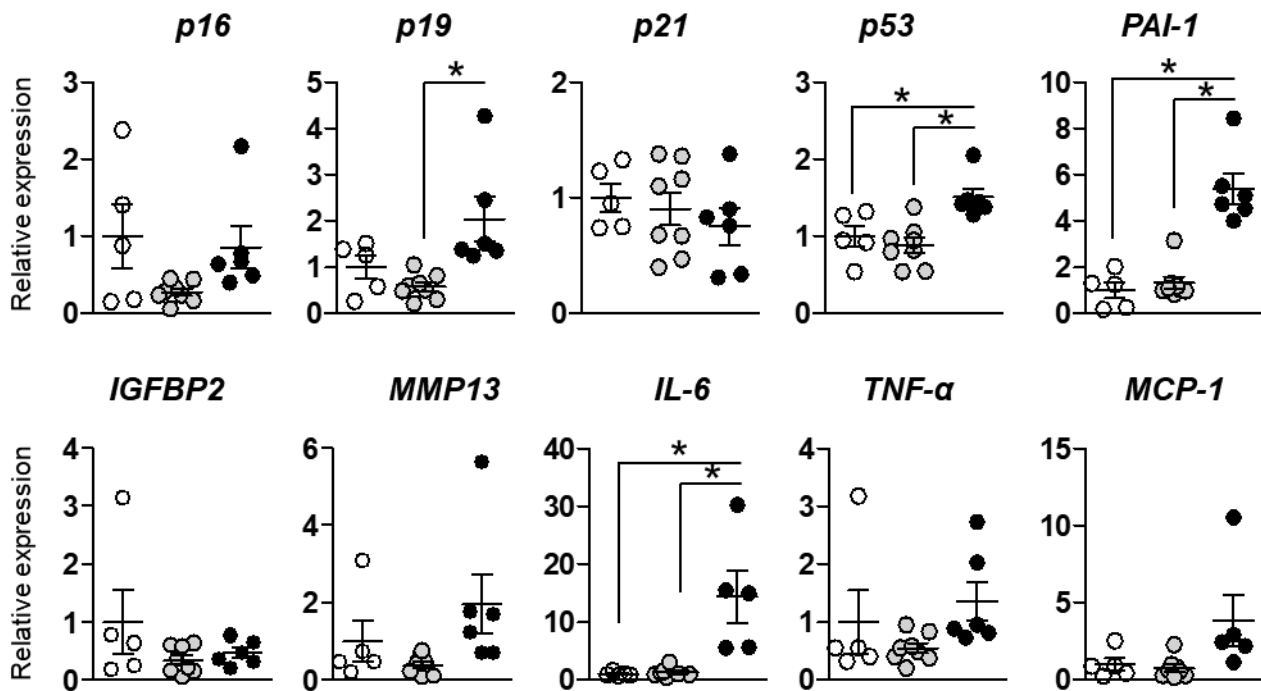
○ WT ○ AT2 KO ● AT2/Mas KO

(b)

Tibialis anterior muscle



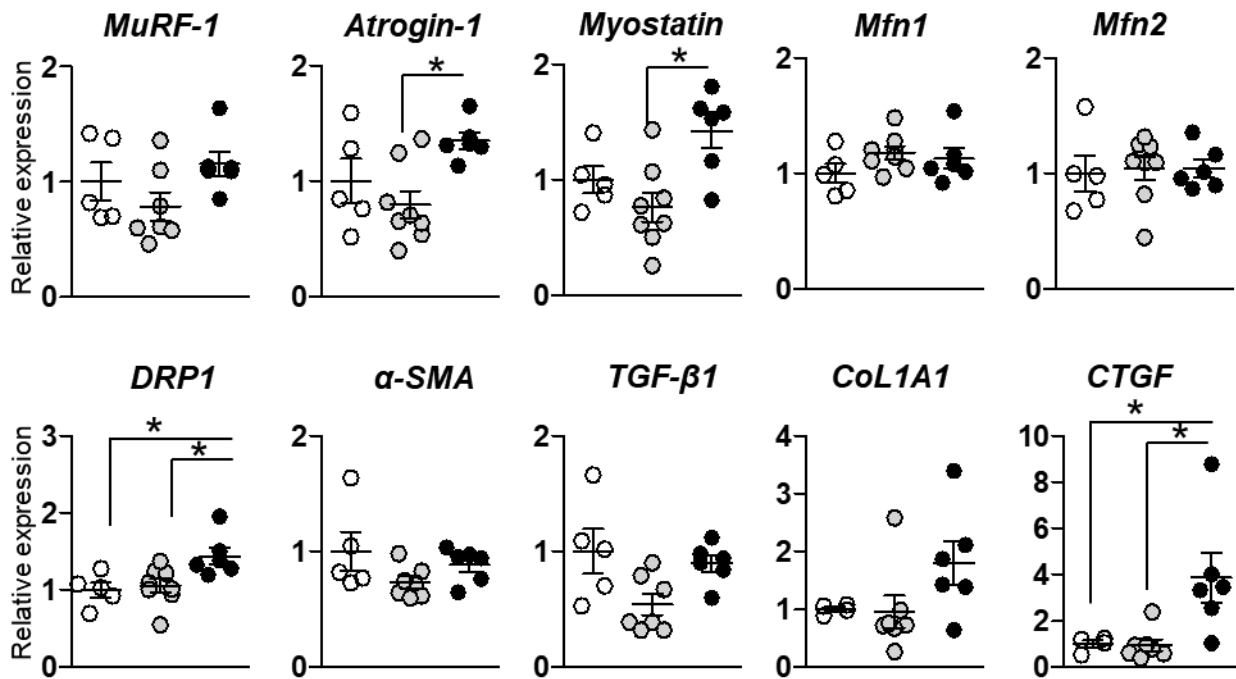
Gastrocnemius muscle



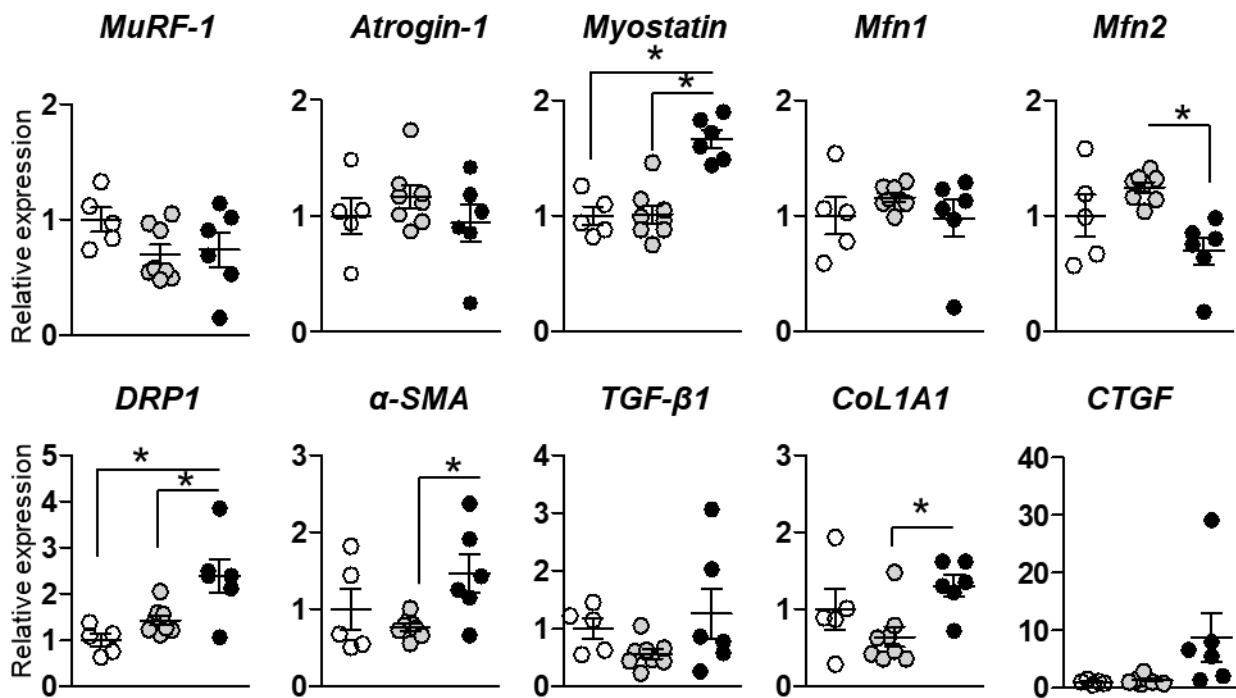
○ WT ○ AT2 KO ● AT2/Mas KO

(c)

Tibialis anterior muscle



Gastrocnemius muscle



WT

AT2 KO

AT2/Mas KO

RT-qPCR analysis of age-induced changes in genes associated with RAS, aging, inflammation, mitochondrial function, and fibrosis in the tibialis-anterior muscle and gastrocnemius muscle in mice.

Quantitative estimation of the expression levels of genes associated with RAS (a), aging and pro-inflammatory senescence-associated secretory phenotype (b), and muscle-specific gene markers of senescence, mitochondrial function, and fibrosis (c), relative to GAPDH expression in the tibialis-anterior muscle and gastrocnemius muscle.

Differences were analyzed with a one-way ANOVA using the Bonferroni post-hoc test.

*, $p < 0.05$

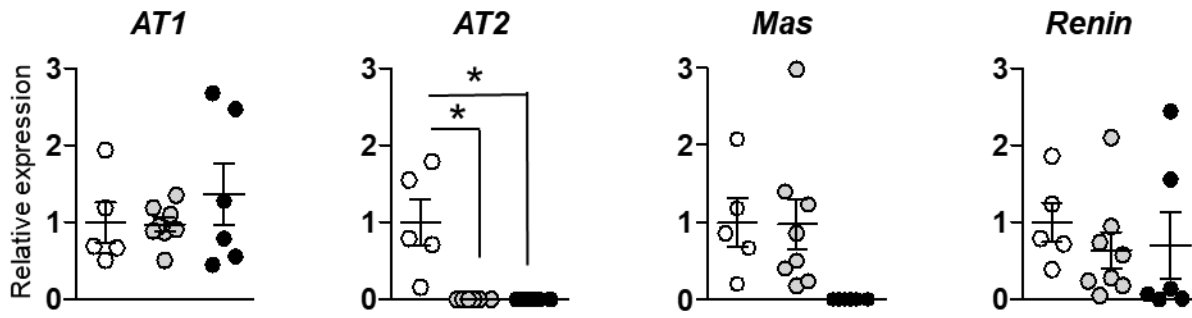
No significant difference was observed among the groups otherwise indicated.

WT, Wild-type; KO, knockout

Fig. S7

(a)

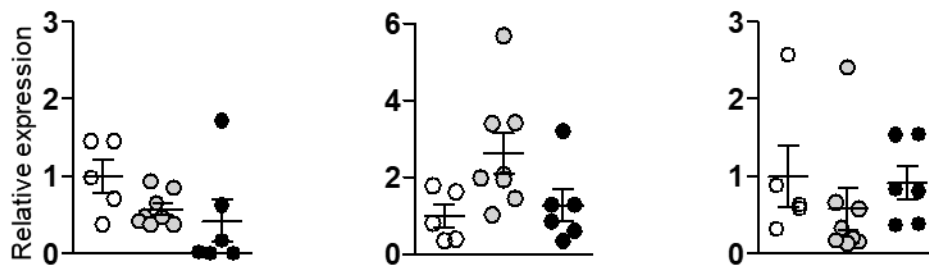
Liver



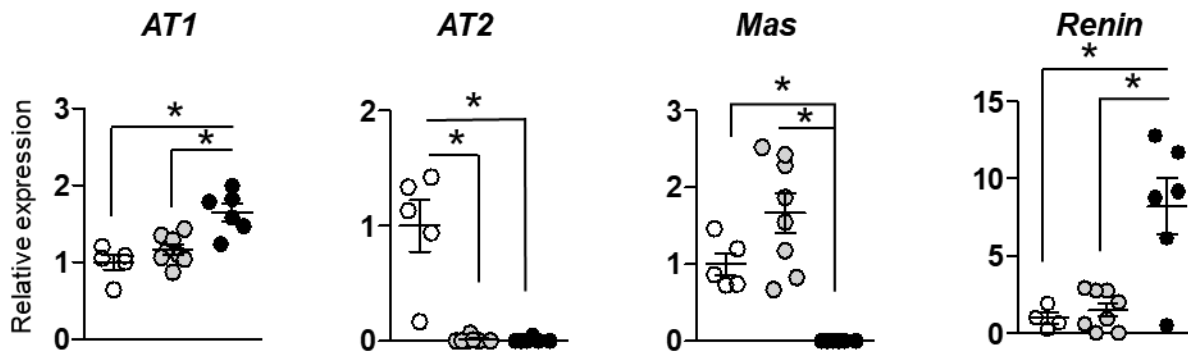
Angiotensinogen

ACE

ACE2



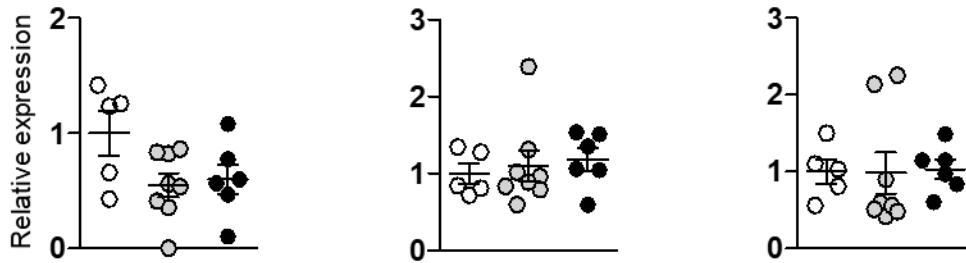
Heart



Angiotensinogen

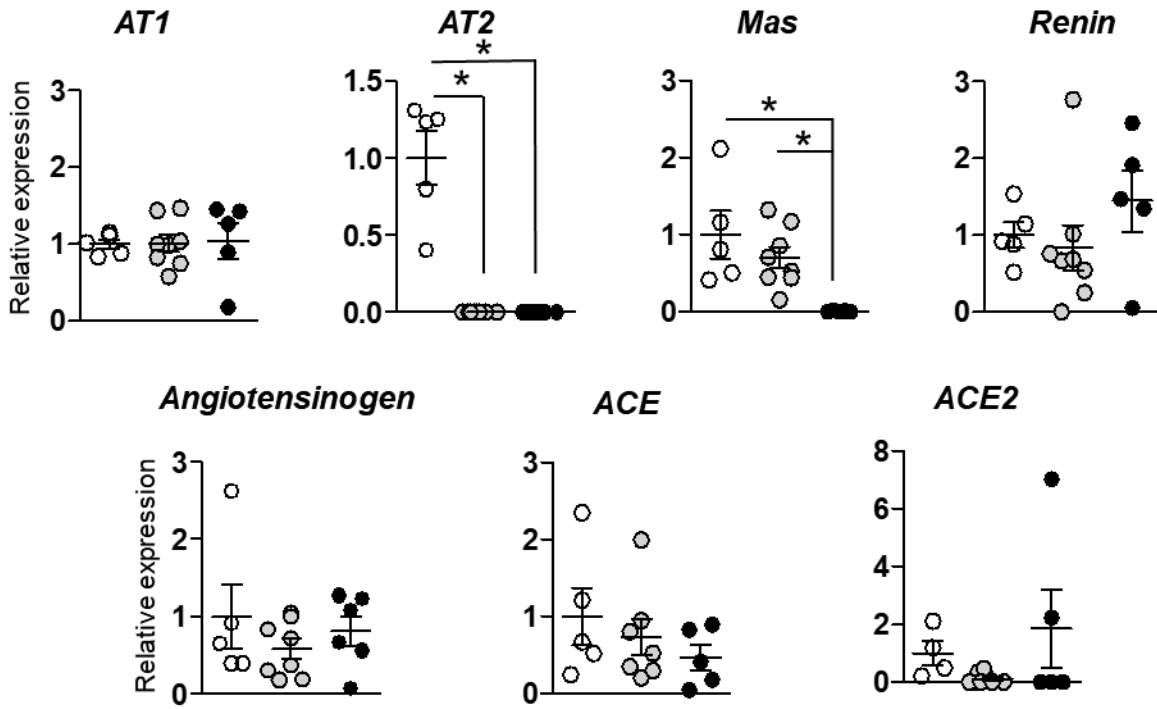
ACE

ACE2



○ WT ○ AT2 KO ● AT2/Mas KO

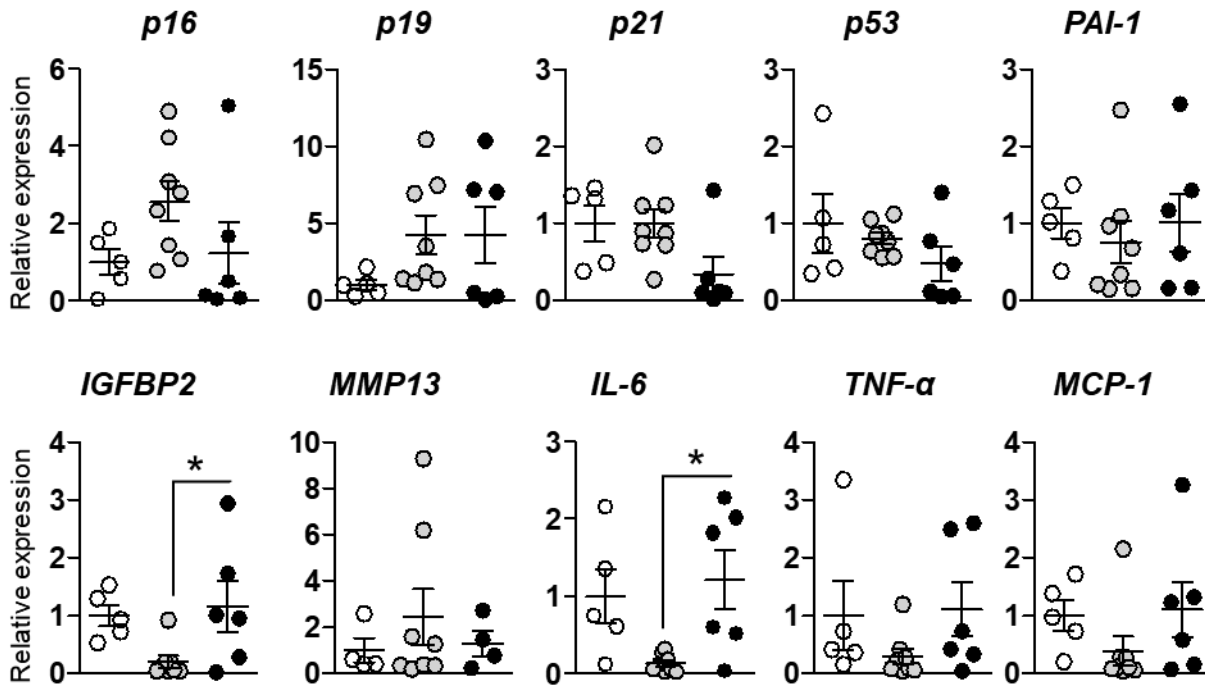
Adipose tissue



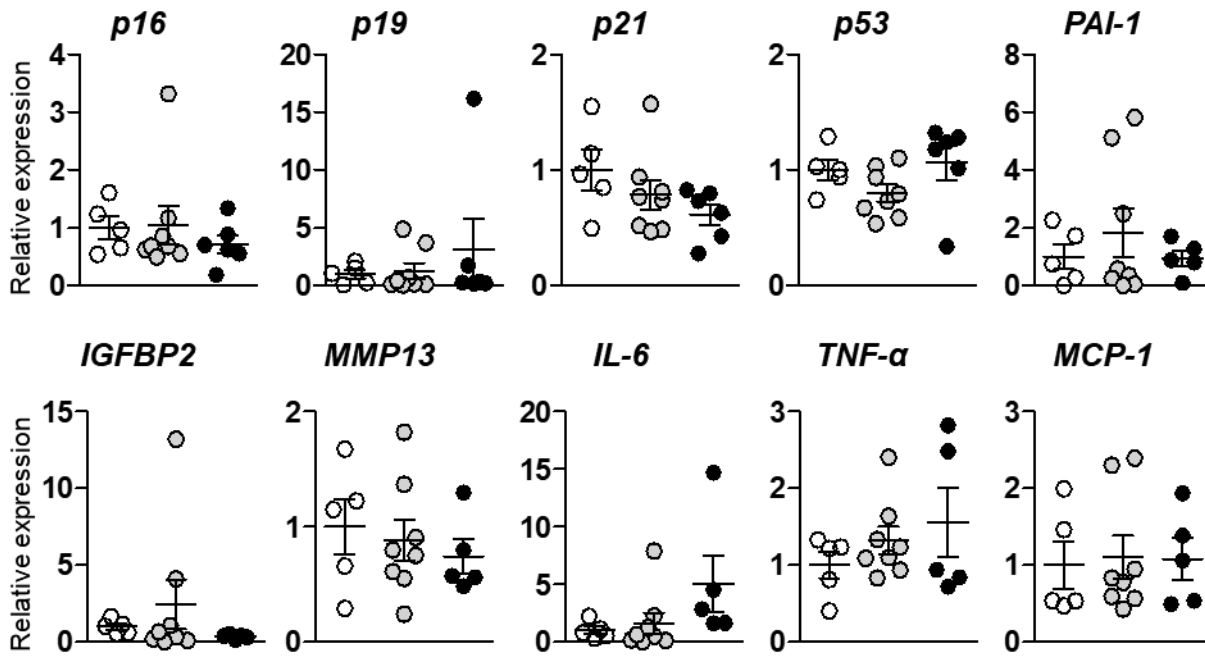
○ WT ○ AT2 KO ● AT2/Mas KO

(b)

Liver

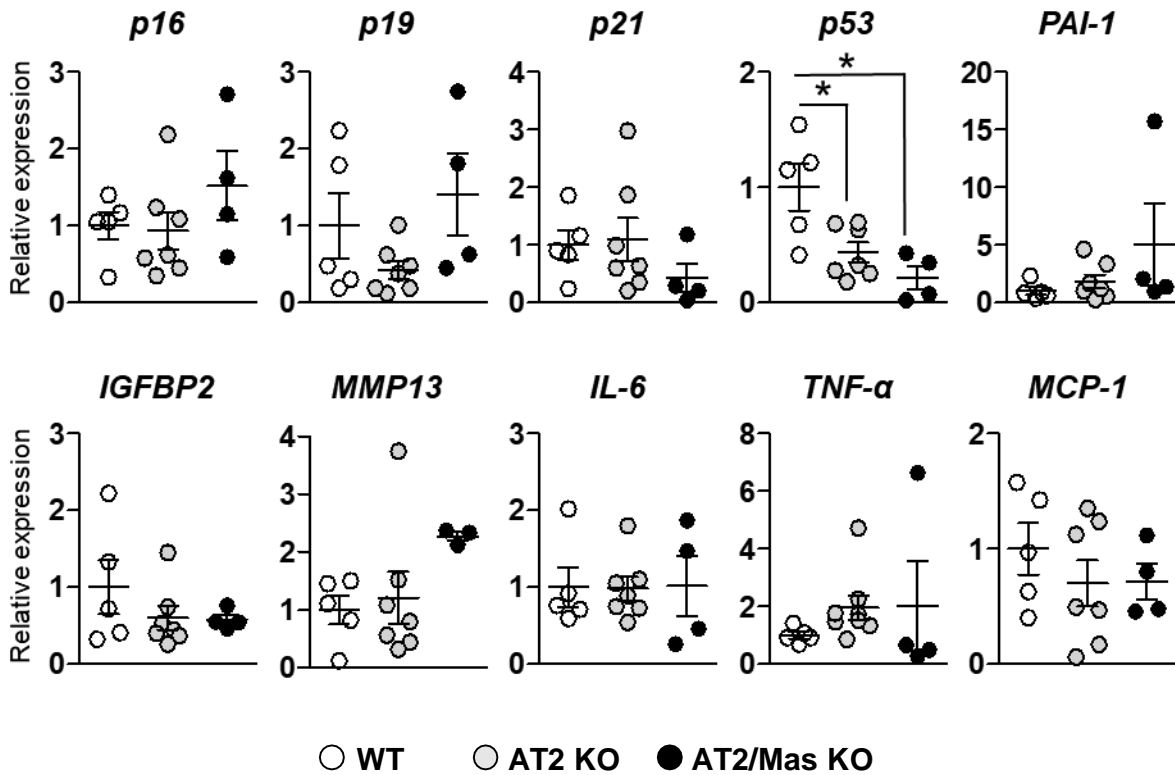


Heart



○ WT ○ AT2 KO ● AT2/Mas KO

Adipose tissue



RT-qPCR analysis of genes associated with RAS, aging, inflammation, and fibrosis in tibialis anterior muscles, heart, and adipose tissues in old mice.

Expression of genes associated with RAS (a) and aging and proinflammatory senescence-associated secretory phenotype (b) relative to *GAPDH* expression in liver anterior muscles, heart, and adipose tissues.

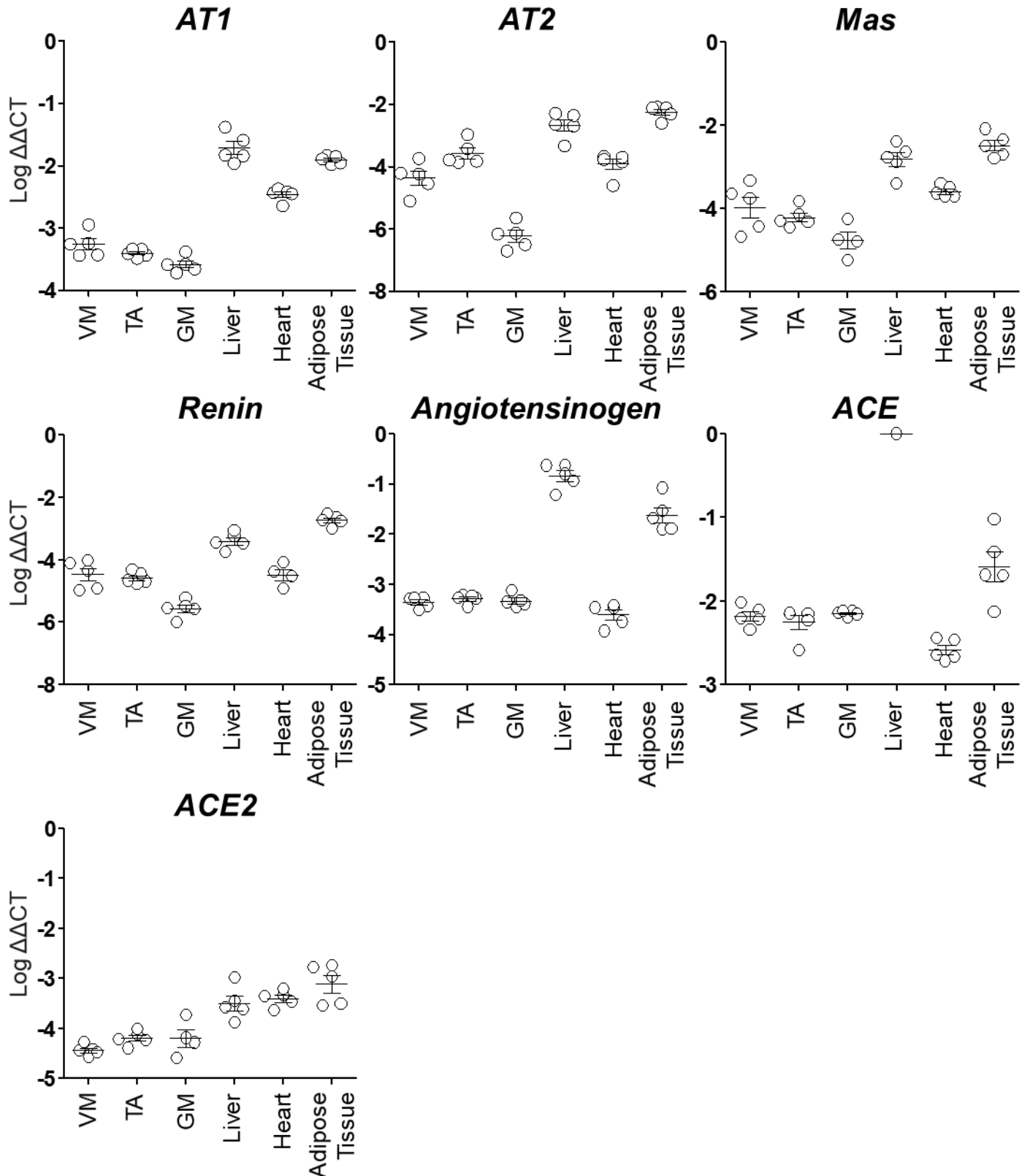
Differences were analyzed with a one-way ANOVA using a Bonferroni post-hoc test.

*, $p < 0.05$

No significant difference was observed among the groups otherwise indicated.

WT, Wild-type, KO, knockout

Fig. S8



Relative abundance of genes associated with RAS in muscles, liver, heart, and adipose tissue in 24 month-old wildtype mice.

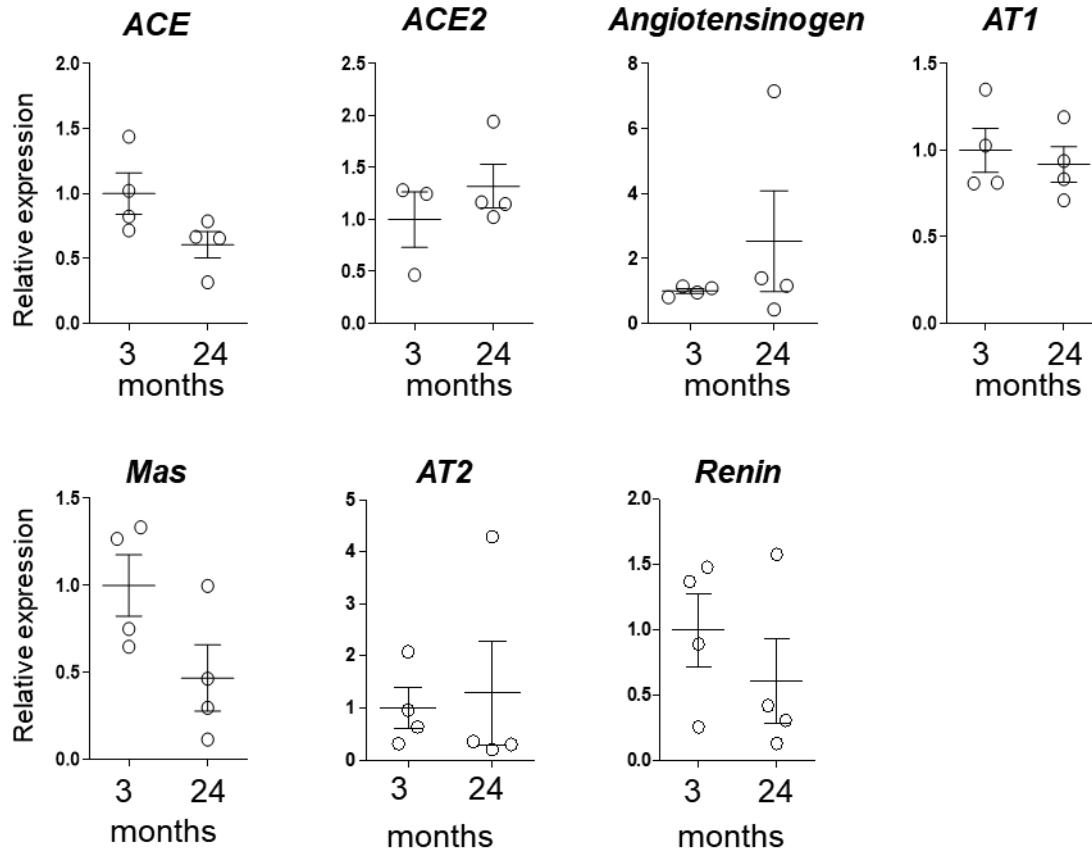
Quantitative estimation of the expression levels of genes associated with RAS.

Comparison of the expression levels of genes associated with RAS across the organs.

Y-axis represents log-transformed $\Delta\Delta$ Ct of each gene normalized to 18S.

VM, vastus muscle; TA, tibialis anterior muscle; GM, gastrocnemius muscle

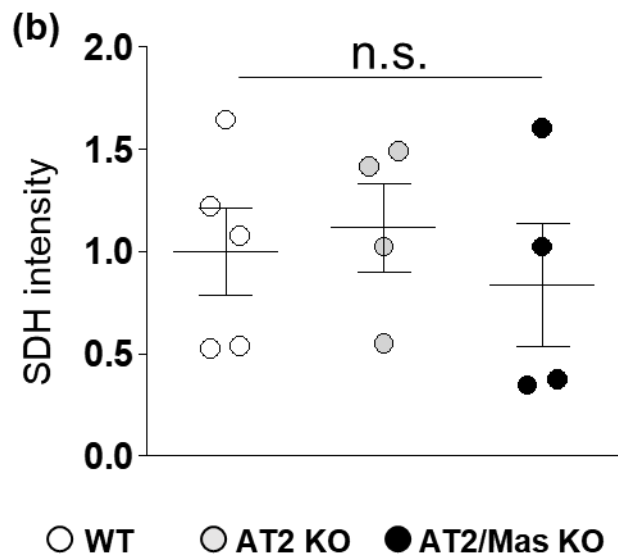
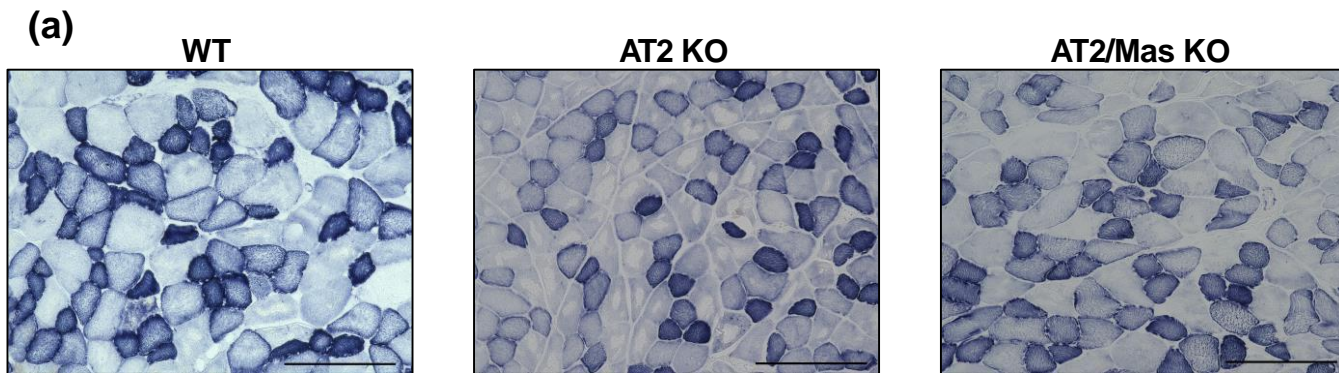
Fig. S9



Aging associated changes in the expression of the renin-angiotensin system (RAS) components in tibialis anterior muscles in mice.

Expression of genes associated with RAS in tibialis anterior muscles of young (3-months old) and aged (24-months old) wildtype mice, relative to *GAPDH* expression. No significant difference was observed between the age-groups analyzed by a Student's t-test.

Fig. S10



Succinate dehydrogenase (SDH) activities of the vastus muscles

Representative SDH-stained sections of the vastus muscle in each group of mice (a).

Average value and distribution of SDH intensity. Differences were analyzed with a one-way ANOVA using a Bonferroni post-hoc test.

n.s., not significant

Scale bars: 200 μ m.